Seeding Induced Assembly of Ionic-Complementary Peptide EAK16-II

By

Sukhdeep Singh Dhadwar

A thesis

presented to the University of Waterloo

in fulfillment of the

thesis requirement for the degree of

Master of Applied Science

in

Chemical Engineering

Waterloo Ontario Canada 2004

AUTHORS DECLARATION FOR ELECTRONIC SUBMISSION OF A THESIS

I herby declare that I am the sole author of this thesis. This is a true copy of the thesis, including any required final revisions, as accepted by my examiners.

I understand that my thesis may be made electronically available to the public.

ABSTRACT

Seeding is an important variable in controlling or directing the assembly of peptides. The presence of impurities, responsible for creating a 'dip' in the surface tension versus peptide concentration profile, is used to determine the critical aggregation concentration (CAC). This phenomenon is investigated to differentiate crude and high purity EAK16-II peptide. The purified peptide did not show this 'dip' and clearly indicated a critical aggregation concentration for EAK16-II at 0.09 mg/mL by surface tension measurements. Conversely, a surface tension 'dip' is clearly observed for the crude EAK16-II peptide. Atomic Force Microscopy imaged the nanostructures of aggregates. The presence of impurities induces fibre formation below the CAC.

This study provides information about the seeding effect of peptide assembly at low concentrations as well as the modification of surface activity of assembled peptide particles. Alanine, glutamic acid and lysine were used as model seeding agents to simulate the seeding phenomenon and better understand the nucleation mechanism of peptide assembly. All amino acid monomers were able to induce fibre formations at low peptide concentrations. However, only glutamic acid and lysine were able to produce the surface tension dip profile observed in the crude peptide. This information may be of importance in understanding fibrillogenesis occurring in conformational diseases and other biomedical applications including drug delivery.

ACKNOWLEDGMENTS

I would like to thank the members of the interfacial engineering group for their support. I want to give special thanks to Professor Dr. Jean Duhamel for the collaboration on this project. Finally, I would like to thank Dr. Pu Chen, my supervisor, for his guidance and providing me with this great research opportunity.

TABLE OF CONTENTS

LIST OF TABLES

LIST OF ILLUSTRATIONS

1.0 INTRODUCTION

Nanotechnology has been one of the most rapidly developing areas in science and engineering in the past decade[1-9]. This has been made possible by the advancement of sensitive analytical techniques such as Atomic Force Microscopy (AFM). The major achievement in nanotechnology is the reorientation of contemporary manufacturing processes: the radical shift from 'top-down' (an approach starting from large scale materials) to 'bottom-up' approach. The key component in the bottom up approach is self-assembly. This involves the careful design of molecules that can self-assemble without external forces to form nano/microstructures. This indigenous engineering route is habitually adopted in nature, permitting establishment of supramolecules such as DNA, silk fiber, spider webbing, and 3D protein gel produced by the Hagfish[10]. Synthetic compounds being explored utilize these natural manufacturing processes.

1.1 Self-assembly

Molecular self-assembly is the spontaneous organization of molecules under near-thermodynamic equilibrium conditions into structurally well-defined and stable arrangements through non covalent interactions, such as hydrogen bonding, electrostatic attractions, and van der Waals interactions[10,11]. Frequently, molecular self-assembly relies on chemical complementarity and structural compatibility[10,12]. These fundamentals are necessary for the design of the molecular units required for the fabrication of functional macrostructures (Figure 1-1).

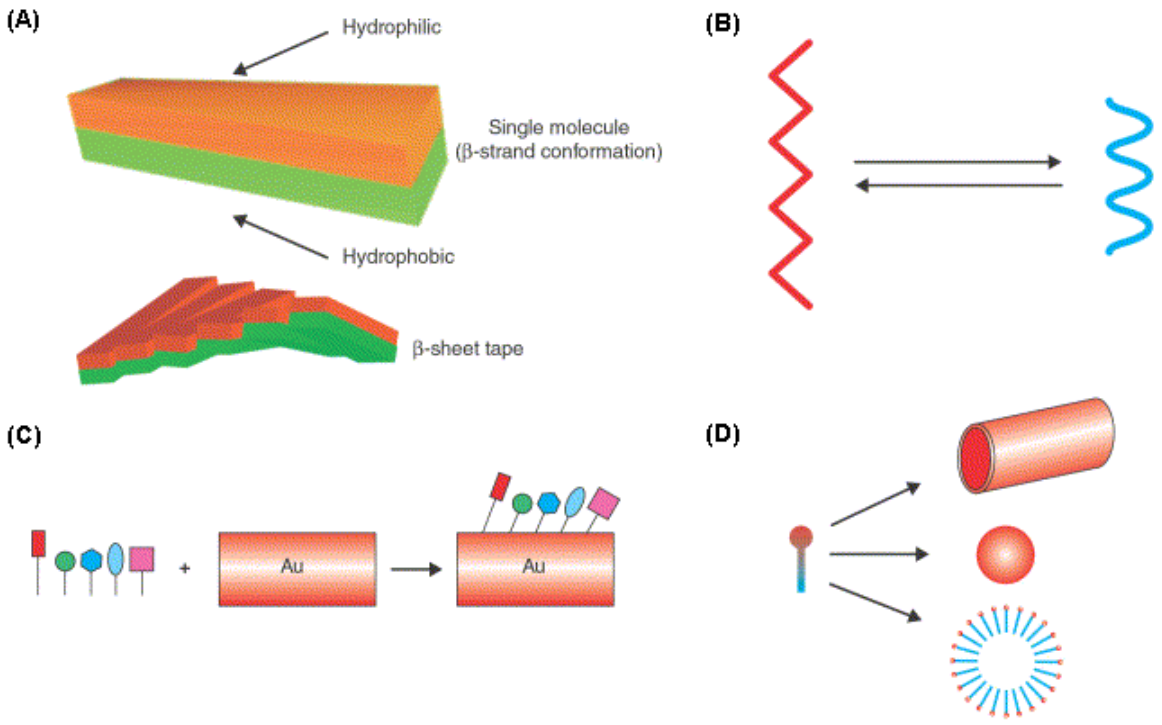

Figure 1-1 Various types of self-assembling peptide systems[13]: (A) β-strand self-assembling peptides and their twisted tape-like nanostructures; (B) self-assembling peptides with the ability of structural transition between α-helix and β-sheet; (C) surface-binding peptides for biological surface patterning; (D) surfactant-like peptides forming nanotubes and nanovesicles.

Peptides, which are short protein sequences, are promising biomaterials in nanotechnology due to their simplicity and diverse functionality. Peptides can be easily designed and synthesized for specific nanoscience research, unlike proteins, which are large and complex[13-15]. Rather than studying the functionality of a particular protein as a whole, the same goal can be achieved by investigating a small section of peptide chains in the protein[16,17]. This approach has been used to gain an understanding of amyloid fibrillogenesis in protein misfolding diseases[16,17].

1.2 Ionic-Complementary Peptides

Ionic-complementary peptides have been studied since the early 1990s[18,19]. Initially the research on these peptides mainly focused on the effect of ionic-complementarity on the a-helix-to-β-sheet secondary structure transition[18-20]. Later, this research was expanded to investigate protein chain folding and the conformational change of the amyloid peptides[21,22].

This new class of peptides was discovered during the analysis of the ZDNA binding protein in yeast which revealed an unusual 16 amino acid sequence with repetitive polar and nonpolar residues, AEAEAKAKAEAEAKAK[23-25]. These peptides are referred to as molecular Lego. Its secondary structure arranged into ß-sheets instead of forming a-helix as predicted by computer simulation[24]. These peptides could also form membrane-like structures. The unique molecular structure with alternating hydrophobic and hydrophilic residues leads to an amphiphilic structure. This unusual amphiphilic structure results in molecular self-assembly to form β-sheets and further aggregate into membranes. In addition, the alternating positive and negative charge distribution results in charge complementarity which is believed to facilitate self-assembly[26-28]. With amino acid sequence originating from living organisms, these self-assembling peptides are biocompatible[29] and biodegradable[30] with promising properties essential for biological applications[13,15].

EAK16 is a typical member of the ionic-complementarity self-assembling peptide family (Table 1-1). It contains three amino acids (alanine, glutamic acid and lysine) connected into a well-defined sixteen long sequence of amino acids[31]. This class of self-assembling peptides can have different charge distributions denoted as I, II, III, and IV etc., according to the sequence of alternating charges[32] (see section 2.2). Type II is characterized by two negative and two positive charges in sequence $(--++--++)$ as shown in Figure 1-2. Instead of exhibiting a

hydrophobic tail and a hydrophilic head as in the case of surfactants, EAK16 has a hydrophobic side and a hydrophilic side. Due to this unique molecular structure, one would expect that the self assembly of such peptides would be different from micellization of most surfactants [25]. This is observed in the formation of stable structures formed by electrostatic interactions from the ionic-complementary residues.

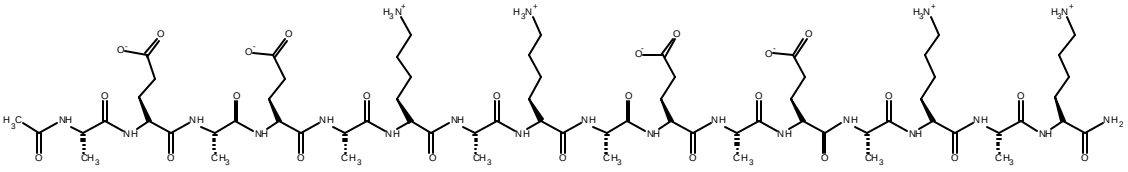

$$AcN-A\overset{-}{E}A\overset{-}{E}A\overset{+}{K}A\overset{+}{K}A\overset{-}{E}A\overset{-}{E}A\overset{+}{K}A\overset{+}{K}-CNH_2$$

Figure 1-2 Chemical structure of an ionic-complementary self-assembling peptide – EAK16-II. It contains alternating hydrophobic (alanine, A) and hydrophilic (glutamic acid, E and lysine, K) residues in sequence, which generates a unique amphiphilic structure with a hydrophobic region on one side and a hydrophilic one on the other. The charged residues are arranged in a fashion as type II, $--++--++$, where pairs of negatively (E) and positively (K) charged side chains alternate in sequence.

The versatility of this class of peptides is due to the ease of its molecular design[15]. Firstly, the charge distribution can be altered resulting in different types of peptides such as type I, II, III, or IV etc. The second feature is the ease at which this peptide family can be expanded with the same charge distribution but with the use of different amino acids. Also, modification of the chain length from 8 to 32 amino acids in sequence yields many more variations (see Table 1). These peptides have shown great importance in molecular self-assembly and potential for nanotechnology [19,21,22,26,33,34].

Table 1-1: Ionic-complementary self-assembling peptides studied by MIT[15,35,36] and our group

Name	Charge distribution Sequence (n ® c)	Type	Structure
	+ − + − + − + −		
RADA16-I	n- RADARADARADARADA -c	I	β
	+ − + − + − + −		
RGDA16-I	n- RADARGDARADARGDA -c	I	r.c.
	+ − + −		
RADA8-I	n- RADARADA –c	I	r.c.
	+ + − − + + − −		
RAD16-II	n- RARADADARARADADA -c	II	β
	+ + − −		
RAD8-II	n- RARADADA –c	II	r.c.
	− + − + − + − +		
EAK16-I	n- AEAKAEAKAEAKAEAK -c	I	β
	− + − +		
EAK8-I	n- AEAKAEAK –c	I	r.c.
	+ − + − + − + −		
KADA16-I	n- KADAKADAKADAKADA -c	I	β
	+ − + −		
KADA8-I	n- KADAKADA –c	I	r.c.
	− − + + − − + +		
EAH16-II	n- AEAEAHAHAEAEAHAH -c	II	β
	− − + +		
EAH8-II	n- AEAEAHAH –c	II	r.c.
	− − + + − − + +		
EFK16-II	n- FEFEFKFKFEFEFKFK -c	II	β
	− + − + − +		
EFK12-I	n- FEFKFEFKFEFK -c	I	β
	− + − +		
EFK8-I	n- FEFKFEFK –c	I	β
	+ − + −		
KFE8-I^{T}	n- KFEFKFEF –c	I	β
	+ − + −		
KFE8-I	n- FKFEFKFE –c	I	β
	+ − + − + −		
KFE12-I	n- FKFEFKFEFKFE -c	I	β
	+ − + − + − + −		
KFE16-I	n- FKFEFKFEFKFEFKFE -c	I	β
	− − + + − − + +		
ELK16-II	n- LELELKLKLELELKLK -c	II	β
	− − + +		
ELK8-II	n- LELELKLK –c	II	β.
	− − + + − − + +		
EAK16-II	n- AEAEAKAKAEAEAKAK -c	II	β
	− − + +		
EAK8-II	n- AEAEAKAK –c	II	r.c.
	+ + + + − − − −		
KAE16-IV	n- KAKAKAKAEAEAEAEA -c	IV	β
	− − − − + + + +		
EAK16-IV	n- AEAEAEAEAKAKAKAK -c	IV	β

β: β-sheet; α: α-helix; r.c.: random coil; N/A not applicable.

1.3 Seeding Agents

The presence of seeding agents or impurities has the ability to affect the peptide assembly. This affect may occur through alterations in structural conformation, chemical bonding, or other types of interactions. This effect is examined in more detail in this study to gain a better understanding of the assembly process and hopefully provide a means of controlling or directing the assembly process. Many neurological disorders such as Alzheimer's, Parkinson's and prion diseases, show strong relations to deposition of amyloid fibrils[37]. Thus, finding inhibitors to the assembly of stable fibrils may lead to a possible cure for neurological disorders. Alternatively, inducing fiber formation may be relevant to the creation of desired peptide structures such as those used in tissue engineering or drug delivery.

1.4 Objectives

The objectives of this research are:

A. to study the effects of peptide impurities in self-assembly.

B. to understand the seeding mechanism of EAK16-II assembly.

C. to study ways of controlling or directing peptide assembly.

2.0 LITERATURE REVIEW

2.1 Self-assembly Peptides

Synthetic self-assembling peptides are derived from segments of naturally occurring proteins or through biomolecular design, which have the common feature of the capability of self-association in aqueous solution. These peptides have received a great deal of attention from biomaterial and nanoscience researchers because they can be engineered to form a wide variety of nanostructures and hold considerable promise for a broad range of applications[13-15,38]. One major research focus has been on amyloid fibrillogenesis, which has been hypothesized as a primary contributor to some debilitating neurological disorders, such as Alzheimer's, Parkinson's, and Prion diseases[17,39].

An understanding of amyloid fibrillogenesis is essential for the development of peptide folding inhibitors and treatments for such diseases. This understanding can be achieved by studying the self-assembly of proteins and their peptide determinants[37,40-46]. Many other amyloid systems have been developed as alternatives to investigate conformational diseases with the use of non-disease related peptides[26,47,48]. Apparently, both ordinary peptides and protein can form amyloid fibers if the conditions are favorable[47,49]. This observation has reinforced amyloid fibrillogenesis research on designed self-assembling peptide systems[50-55]. The complete understanding of peptide self-assembly may provide molecular therapies for conformational diseases[56,57].

Synthetic self-assembling peptides can be used to build supramolecules through careful molecular design. Amphiphilic peptides, which contain both hydrophobic and hydrophilic regions, self-assemble to form a-helices, β-sheets, or random coils. Peptide self-assembly is based on the intrinsic propensity of the amino acid residues to form α-helices, β-sheets or random

coils and their arrangements. The positioning of the individual residues is reported to be a major determinant of secondary structure formation[58]. As a result, one can design a peptide to form a desired secondary structure by carefully choosing and arranging the sequence of amino acids. This allows the construction of a diverse set of nanostructures, each with a particular function[59,60]. Zhang et al. have shown various types of self-assembling peptide systems (Table 1) with the capability to form twisted β-sheets, to undergo conformational changes, to bind with surfaces, or to be used to construct nanotubes and nanovesicles[13,15]. Each of these supramolecular formations is governed by the intrinsic properties of the peptide unit.

The self-association of peptides into insoluble macroscopic membranes could also be considered as a model system for studying insoluble macrostructures, which have been found in many neurological disorders, such as Alzheimer's disease[25,31,36,61]. The macroscopic membranes or plaques can interfere with or even prevent cell-to-cell communications, which results in neurological disorders. One well-known self-assembling biomolecule is the amyloid ß-protein (Aß), which has been found to be an important factor in the cause of Alzheimer's disease[56]. However, the self-assembly process of Aß is so complicated that it is still not fully understood. Rather than looking at the completed Aß molecule, the study of the self-assembly of shorter peptides may be an alternative[62,63]. These peptides could be a model system that would enable the finding of inhibitors that prevent fibrillogenesis and possibly provide therapy to neurological disorders.

2.2 Ionic-Complementary Peptides

Over the past five years, a new class of peptides— ionic self-complementary, amphiphilic peptides have been actively studied[13,25,31,36,64-67] (Table 1-1). These peptides not only possess significant biological functions but also have surfactant-like characteristics due to their unique amino acid sequences. Since its discovery, this new class of peptides has been used in many areas of science and engineering, including molecular medicine and nano-biotechnology[32]. These molecules have been shown to form self-assembling scaffolds for tissue engineering[61,67], and proven to be biocompatible when injected by themselves or in conjugated form into rabbits, rats and goats[68].

The first member of ionic-complementary peptide family discovered by Zhang et al (1993) was EAK16-II, a 16 amino acid peptide segment originating from a ZDNA binding protein[23,25]. EAK16-II contains alternating hydrophobic and hydrophilic amino acids residues. This repetitive arrangement of amino acids, imparts an amphiphilic property to the peptide. Instead of exhibiting a hydrophobic tail and a hydrophilic head as surfactants do, EAK16-II has a hydrophobic side and a hydrophilic side. Due to this unique molecular structure, one would expect the self-assembly of such peptides to be different from the micellization of most surfactants[64]. Zhang et al demonstrated this point in their initial work on EAK[25]. This peptide forms a β-sheets rather than an a-helix. The stable supramolecular structure is most likely caused by the effect of electrostatic interactions from the ionic-complementary residues.

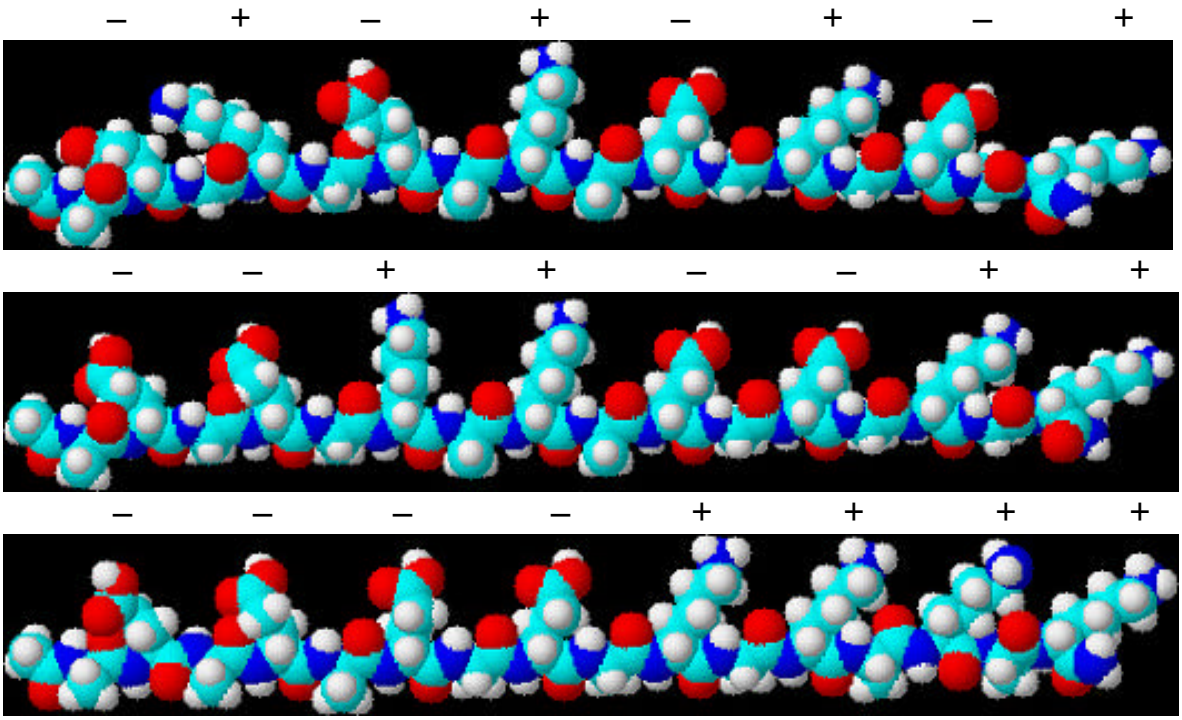

Figure 2-2 The three-dimensional molecular model of type EAK16s. The top, middle, and bottom scheme represents the molecular structure of EAK16-I, EAK16II, and EAK16-IV with a charge distribution of $-+-+-+-+$, $--++--++$, and $----++++$, respectively. The length of the backbone of EAK16s is around 7 nm while the width ranges from 0.3 to 0.7 nm (image generated from ACD/3D freeware, Toronto, ON, Canada).

Ionic-complementary peptides are characterized by an alternating arrangement of negatively and positively charged residues. Because of these ordered charge sequences, unique elestrostatic interactions are derived, which the peptides use, in addition to the usual hydrogen bonds or Van der Waals' forces, to control their molecular self-assembly. In order to have ionic-complementarity, the distribution of the charges should follow certain patterns. Their charge distribution can be altered through simple molecular design, resulting in several types of the

peptides, such as type I, $-+$; type II, $--++$; type III, ---+++ and type IV, $----++++$[15,35,36]. Figure 2-2 shows the results of a sequence design based on the same components (E, A, and K) that generate EAK16-I, EAK16-II and EAK16-IV. It is possible to design additional ionic-complementary peptides by repeating or combining these charge distribution types. The combination of different types of charge distribution in a single peptide, however, may render the study of its self-assembly far too complicated, in spite of the fact that the combination may duplicate the actual charge distribution of a living system.

2.3 Single Molecular Peptide Structure

Through computational simulations, the most stable peptide molecule conformations for EAK16 were determined. The lowest energy conformations are clearly different between EAK16-I, EAK16-II and EAK16-IV. Figure 2-3 shows the "cloud map" of the chain-energy E with respect to the end-to-end distance (aa)[69]. The most stable conformation for EAK16-IV is the hairpin structure, whereas the most stable conformation for EAK16-I is the stretched form. However, EAK16-II has two stable states: a hairpin and a stretched structure. Combining theoretical and experimental approaches, Jun et al. showed that there exists a correlation between single molecule structure and self-assembled nanostructure: EAK16-IV, whose single molecule structure is of a hairpin, formed a globular nanostructure through self-assembly; whereas, EAK16-II, which showed a stretched single molecule structure, formed a fibrillar nanostructure[70].

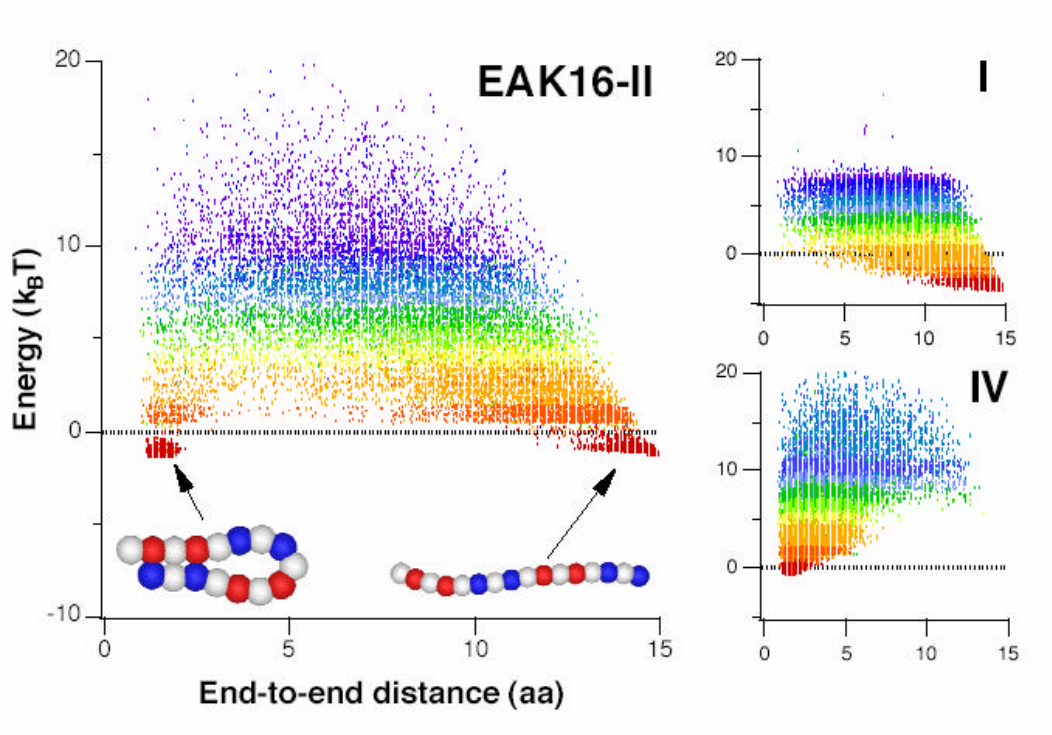

Figure 2-3 The ground energy states of EAK16s as a function of end-to-end distance aa.

2.4 Highly Stable b-Sheet Assemblies

Secondary structures are critical to proper protein folding and peptide self-assembly. There are two essential secondary structures: a-helix and β-sheet. It is believed that the main cause of a-helix or β-sheet formation is intra- or intermolecular interactions through hydrogen bonding[71]. Knowledge of the secondary structure of a peptide is important since it determines high-level structural construction and functionality.

In order to understand the relationship between the secondary structure and the molecular structure, Hecht and his group[58] performed a well-controlled experiment using ionic-complementary peptides. They designed peptides that have the same amino acid compositions but with different charge distributions: α-helical periodicity $(--++--++)$ and β-strand periodicity $(-+-+)$. By this design, they were able to determine that the secondary structure is dominated by periodicity, if the periodicity is different from the intrinsic propensity of the amino acids. This demonstrates the importance of charge distribution in determining peptides' or proteins' secondary structure. However, this is not always the case.

There are few simple rules that can precisely predict the secondary structure from the amino acid sequence. The periodicity of the amino acid side groups provides strong interactions in a specific secondary structure. Since α-helices have 3.6 amino acid residues per turn, separating two amino acids that interact strongly by four residues (i.e. *i, i+4*) may increase the stability of a-helix. Hence, given the charge distribution $--++--++$, the structure of EAK16-II was predicted to be an a-helix by computer simulation. However, this was contradicted by the β-sheet structure of EAK16-II observed by Zhang et al[24]. In a beta-sheet two or more polypeptides chains run along side each other and are linked in a regular manner hydrogen bonds. This is in contrast with an a-helix where all the hydrogen bonds involve the same element of secondary structure. This unexpected β-sheet structure formed by EAK16-II may be caused by the unique amino acid sequence that came

available a number of intermolecular forces including ionic-complimentary electrostatic, hydrophobic, and Van der Walls forces in addition to hydrogen bonding as shown in Figure 2-4.

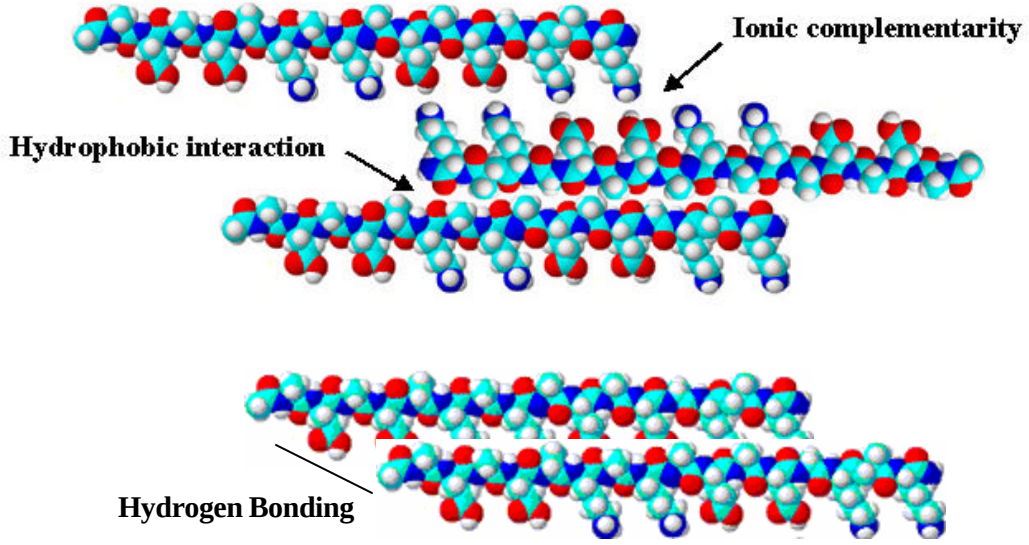

Figure 2-4 A scheme of EAK16-II self-assembly through hydrophobic interaction and ionic-complementarity. In addition to the hydrogen bonding, hydrophobic and electrostatic interactions help to make stable β-sheets.

The β-sheets formed by EAK16-II can further assemble into very stable membrane-like supramolecules. They can withstand high temperatures of up to 90°C for more than 4hr in 1% sodium dodecyl sulfate (SDS) solution[31]. In addition, they are resistant to digestion with several proteases-including trypsin, alpha-chymotrypsin, papain, protease K, and pronase- at a concentration of 100 μg/ml[31]. The membranes are also mechanically stable and can be transferred from one solution to another by means of a solid support[25]. This unusual stability of the membrane is believed to be a consequence of the durable β-sheets. Indeed, the β-sheets

formed by many ionic-complementary peptides are extremely stable under a broad set of physiological conditions and are even impervious to denaturing agents[31].

The ß-sheet structures of EAK16-II are stable over a range of pH values. The sequence has four positively charged (lysine, pKa=10) and four negatively charged (glutamic acid, pKa=4.4) residues in sequence and a calculated pI of 6.71. The pI indicates that the pH value of the isoelectic point at which the peptide carries no net charge. It is anticipated that the charge distribution will be greatly affected at different pH values since some of the charged residues will be neutralized. However, only a small variation in peptide assembly was observed when the pH values were varied from 1.5 to 11[25,27]. This suggests that the secondary structure will not be altered, even when ionic bonding is destroyed by charge neutralization. One explanation for this is that the ionic-complementary residues are able to form strong hydrogen bonds in addition to their ionic interactions. Even though the ionic interactions are lost at extremely low pH values (such as pH 1.5) the non-charged carboxyl groups on the glutamic acid residues are still capable of forming hydrogen bonds with the protonated amino groups on the lysine residues[27].

When the salts were added to the EAK16 II solution, the peptide spontaneously assembled into a membrane. The salts appear have the following order of effectiveness in inducing membrane formation: $Li^+ > Na^+ > K^+ > Cs^+$. Presently, it is not known if the salts act as a catalyst, or if they are somehow incorporated into the membrane (which is more likely). This would not be uncommon, as there are many other examples of monovalent metal ions that promote and stabilize other structures[72].

2.5 Surfactant Micellization and Peptide Assembly

Although the structures of peptide assemblies are different from micelles, surfactant micellization can be used as an analogue for better understanding the self assembly of ionic-

complementary peptides. Surfactants behave differently from other molecules in solution because of their amphiphilic character. Surfactant molecules have two distinct parts; one has an affinity for to the solvent, the other does not. In aqueous systems, the two moieties are usually the hydrophobic head and hydrophobic tail, respectively. The molecular structure of a typical surfactant is shown in Figure 2-5. An amphiphilic molecule can arrange itself at the surface of the water such that the polar part interacts with the water and the hydrophobic tail is held above the surface. The presence of these molecules on the surface disrupts the cohesive energy at the surface and thus lowers the surface tension. Such molecules are called SURFace ACTive AgeNTs or surfactants.

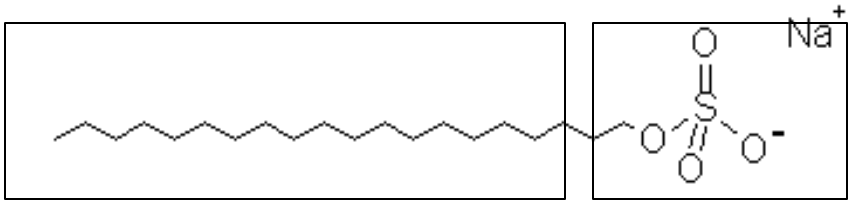

Figure 2-5 Molecular structure of Sodium dodecyl sulphate (SDS). It contains a hydrophilic head and a hydrophobic tail.

These molecules can also arrange into aggregates in which the hydrophobic portions are oriented within the clusters and the hydrophilic portions exposed to the solvent. Such aggregates are called micelles. Micelle formation is highly concentration dependant. Surfactants will not self-associate into micelles until their bulk concentration reaches a certain level. The concentration at which micelles first appear in solution is called the Critical Micelle Concentration (CMC). From in interfacial point of view, surface tension decreases as the

concentration increase because the surfactant molecule absorbs onto the surface. When the bulk concentration reaches the CMC, the surface is entirely packed by the surfactant molecules, therefore the surface tension remains the same and the micelles form.

Self-assembling peptides aggregate in a different manner compared to surfactant micellization, where peptide form open structures like fibril networks in contrast to surfactants which form closed structures such as micelles. This is due to the unique molecular structure of peptide with hydrophobic and hydrophilic sides as shown in Figure 2-6. This also causes the difference of self-association process between peptide aggregation and surfactant micellization.

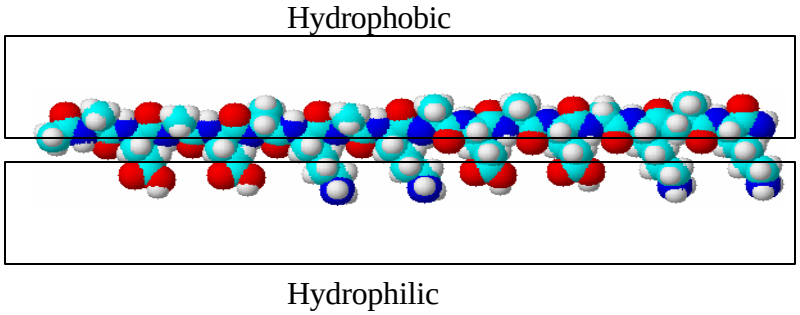

Figure 2-6: Molecular structure of EAK16-II. It contains a hydrophilic side and a hydrophobic side.

The peptide aggregation process occurs through three major interactions: hydrogen bonding, ionic-complementary, and hydrophobic interactions; while the micellization of the surfactants is mainly due to their amphiphilic attribute. Figure 2-7 shows a model of EAK16-II self-assembly. Each peptide molecule first self associates into β-sheets via hydrogen bonding. This has been confirmed by Zhang et al[73]. These β-sheets further interact with each other to form bigger aggregates through their complementary ionic bonds or hydrophobic interactions. This

shows possibility that peptide could aggregate into supramolecules by stacking more/or larger β-sheets, producing an open aggregate structure.

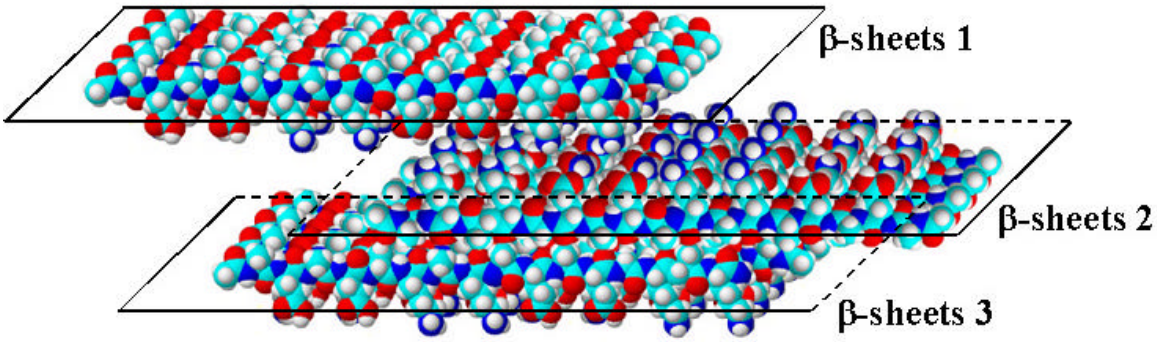

Figure 2-7 A proposed model of EAK16-II self-assembly into β-sheet-based aggregates. It is proposed that the peptides self-assemble in the fashion of anti-parallel to favor the minimum energy state. The layers of β-sheet can stack together through hydrophobic interaction and ionic-complementarity. They can further form fibril-like structures or even membranes.

2.6 EAK16-II Peptide Assembly

Peptide concentration is an important parameter in the control of peptide self-assembly. The concentration dependence of peptide self-assembly is expected to resemble that of surfactants. Applying this concept from micellular systems, one may anticipate that the peptides would be dispersed in a solution below a Critical Aggregation Concentration (CAC) and begin to aggregate at or above the CAC.

Recently, Fung et al reported a CAC value of 60 μM for EAK 16-II (0.1mg/mL)[64]. The experiment was conducted by the Axisymmetric Drop Shape Analysis - Profile (ADSA-P) technique to obtain the surface tension of EAK16-II at different concentrations[64]. The equilibrium surface tension was plotted against the peptide concentration. When the molecules

begin to aggregate from their monomer states, the solution properties are influenced and surface tension reaches a minimum. A 'breaking point' has been seen in the surface tension profile, which is the CAC point (Figure 2-8).

The small depression at the breaking point in the surface tension profile is related to the presence of impurities in the peptide solution. It has been reported that impurities may cause either a lower or higher breaking point[74]. The presence of highly active impurities will cause a lower breaking point, and the presence of less surface active impurities will cause a higher breaking point (see Figure 2-14 on page 27). In addition, the presence of impurities may affect the self-assembly mechanism as well. A large body of work on amyloid fibrillogenesis has shown the importance of impurities in self-assembling peptide systems[17,75,76].

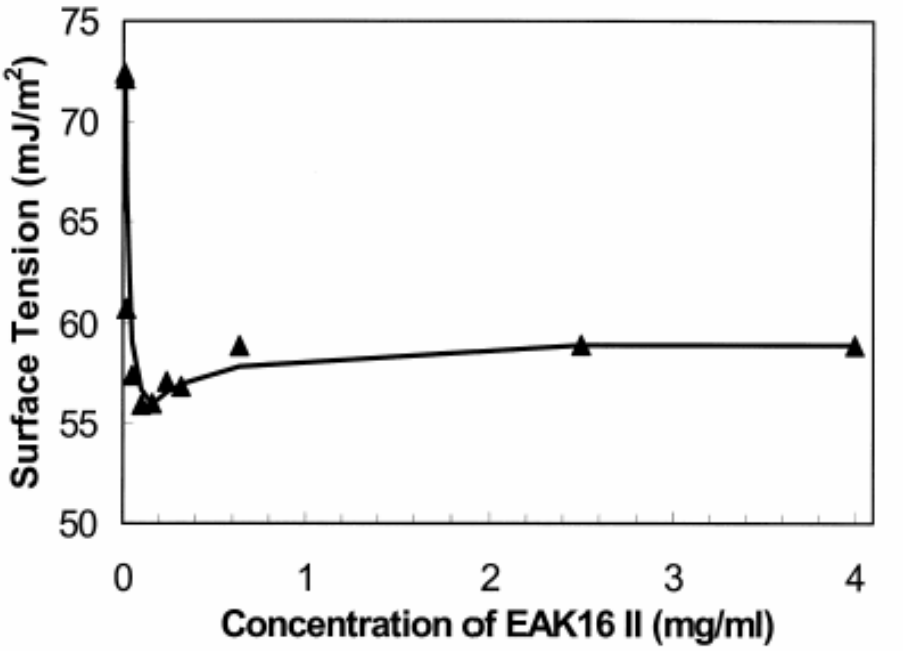

Figure 2-8 Critical aggregation concentration (CAC) of EAK16-II[64]: CAC can be determined by surface tension measurements. The surface tension decreases dramatically down to a minimum, and then increases slightly back to a plateau as the increase of the concentration. The break point of the curve indicates the CAC of EAK16-II.

The formation of self-assembled peptide nanostructures is also concentration dependent. The nanostructure of EAK16-II in water was investigated by AFM and found to differ depending on whether the concentration is above or below the CAC of 0.1 mg/mL (60 μM)[64]. Above the CAC, the EAK16-II formed fiber networks. Isolated filaments and globules were observed at concentrations below the CAC (Figure 2-9). These isolated structures are referred to as protofibrils, defined as intermediates existing prior to the self-assembly of peptides into larger aggregates or fibrils. When the concentration approaches the CAC, both fibrils and protofibrils are observed[64]. A complete understanding of the formation of the two types of protofibrils, filaments and globules, by EAK16-II remains under investigation.

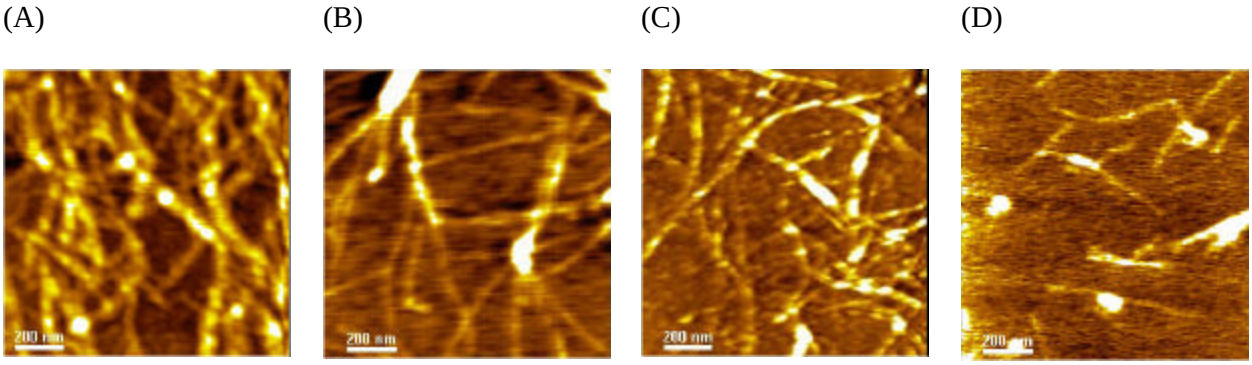

Figure 2-9 Peptide self-assembled nanostructures are concentration dependant[64]: Above the CAC (A) 0.5 mg/mL; (B) 0.2 mg/mL; (C) 0.1 mg/mL (fibril networks); and below the CAC (D) 0.05 mg/mL (filaments and globules) examined by AFM.

The observation of protofibrils at concentrations below the CAC seems to contradict the micellization theory. In micellization, surfactants are present only in monomer form when the concentration is below the CMC. This, however, is not the case for many self-assembly peptides. Peptides such as Aß will aggregate even at concentrations below the CAC, because aggregation

is based on a nucleation mechanism. The nuclei are formed either through the peptides themselves at concentrations above the CAC, or by the impurities present in the solution at concentrations below the CAC. The presence of impurities was confirmed by the surface tension measurements.

The formation of nanostrucutes can be produces by nucleation and micellization pathways. The first step, nanostructure formation, is based on the presence of nuclei in the solutions, which determines which path the peptides will follow. If there are impurities within the solution and the solution is below the critical aggregate concentration (CAC), then seeding takes place to form either filaments or globular aggregates. If there are no impurities and the peptide solution goes above the CAC, then the CAC is what directs the formation of the either filaments or globular aggregates. Both steps of these models, nucleation and aggregation, are time and concentration dependent.

2.7 Controlling Peptide Assembly

Peptide self-assembly may be controlled by the addition of 'self'-inhibitors before peptides start to aggregate. Zhang et al. recently demonstrated that the RADA16-I nanofibril growth can be inhibited by the addition of RADA 8-I peptide, a single unit of RADA 16-I[77]. RADA 16-I forms typical β-sheets spontaneously in aqueous solution, predominately driven by hydrophobic interactions, ionic interactions, and hydrogen bonding. The stable β-sheet can pack together through ionic and hydrophobic interactions to further assemble into long nanofibers with the average length of ~870 nm (Figure 2-10a). On the other hand, RADA 8-I has a random coil structure and does not form nanofibers under identical conditions[77].

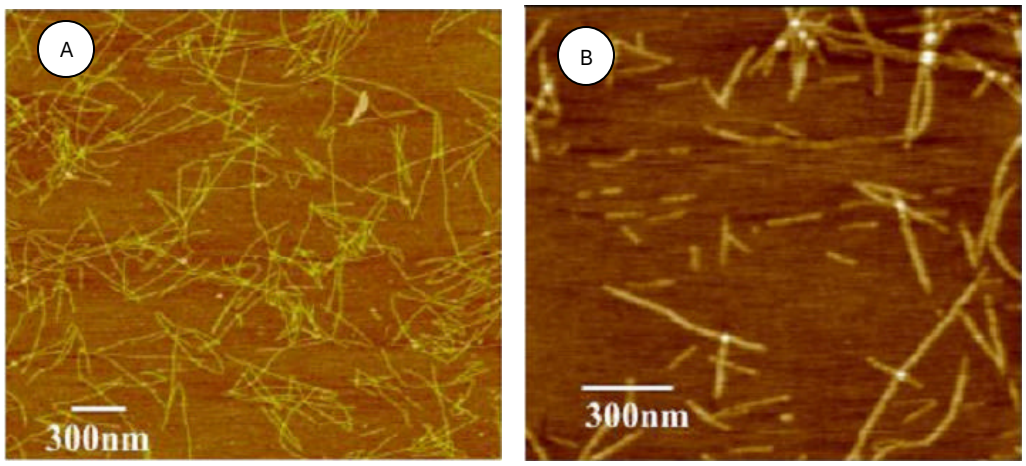

Figure 2-10 Nanofibers of self-assembled from RADA16-I, RADA8-I, and their composite. A) RADA16-I forms a nanofiber network B) RADA16-I and RADA8-I Composite at 1:32 displays more isolated fragments.

When RADA 16-I and RADA 8-I powders are mixed at a stoichiometric ratio of 1:32, AFM scanning of the composite RADA 16-I/RADA 8-I revealed much shorter fiber (150nm) without extensive networks (Figure 2-10b). The average length of the composite nanofiber is approximately 6 times shorter than that of pure RADA 16-I nanofibre.

2.8 Directing Assembly of Peptides

Lormakin et al. proposed a model to describe the aggregation of Aß in a similar self-assembly system[78,79]. The process of Aβ fibrillogenesis is different depending on whether the initial protein concentration is less than or greater than a critical concentration. Above the CAC, a reversible equilibrium between monomer and micelles is rapidly established. Since assemblies are regions of high peptide concentration, it is assumed that they serve as sites for the nucleation of Aß fibrils (Figure 2-11a). Alternative pathways, including heterogeneous nucleation (seeding or impurities), may also exist for the formation of fibril nuclei. When the peptide concentration is

below the CAC, no assemblies are formed and these alternative nucleation pathways predominate. The nuclei provide a core for Aß molecules that can rearrange into fibrils. The elongation occurs by irreversible binding of Aß monomers to the fibril ends (Figure 2-11b).

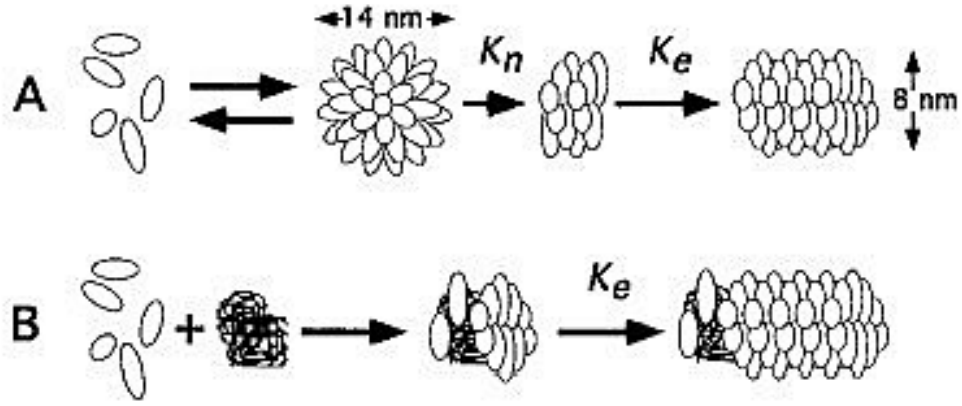

Figure 2-11 Aβ fibrillogenesis at low pH. A: homogeneous nucleation and growth of Aß fibrils at concentrations above the CAC; B: heterogeneous nucleation and growth of Aß fibrils at concentrations below the CAC.

2.9 Peptide Impurities

The EAK16-II peptide, investigated in this study, was manufactured by Fmoc synthesis. The crude peptide contains several impurities including truncated sequences and reagents used in the synthesis process[80-82]. Since the majority of the impurities are truncated sequences; the L-amino acid monomers alanine, glutamic acid, and lysine were used for the purpose of examining the seeding effect on peptide assembly (Figure 2-12).

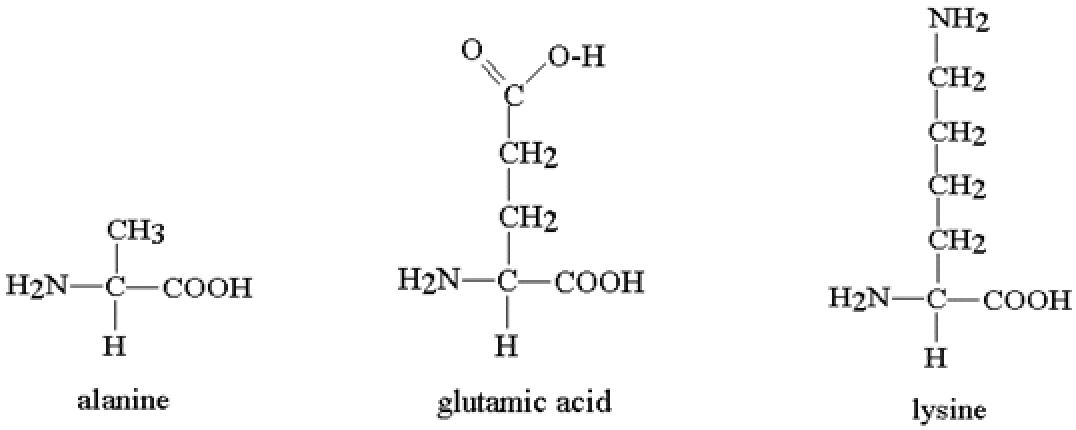

Figure 2-12 Structure of amino acids monomers alanine, glutamic acid and lysine

2.10 Analytical Techniques

2.10.1 Surface Tension

Surface tension is a powerful method to characterize solution containing a given surfactant and determine CMC. This is achieved by measuring surface tension as a function of surfactant concentration.

Axisymmetrical Drop Shape Analysis – Profile (ADSA-P) is a powerful and flexible method to generate information for surface characterization. Measurements can be conducted at different concentrations, temperatures and pressures with high accuracy[83,84] . In addition, dynamic measurements can be made since images of drop shapes are automatically captured and recorded digitally.

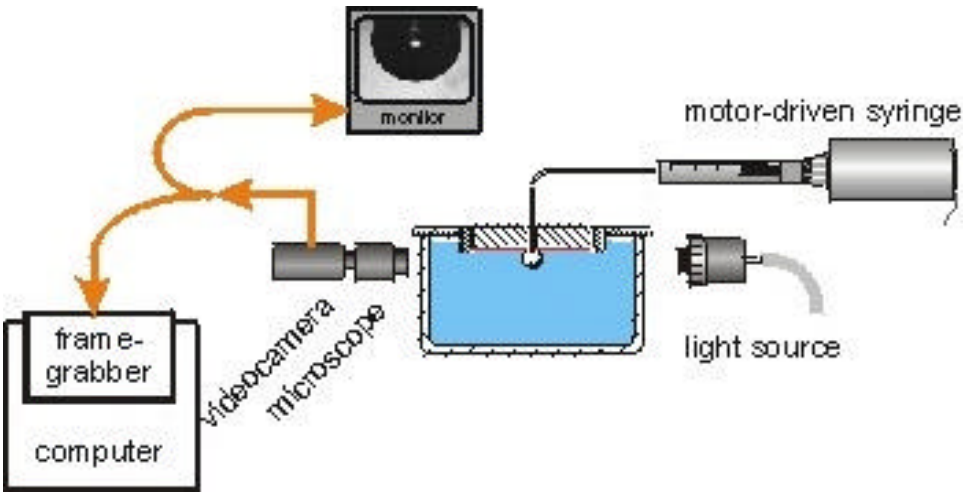

Figure 2-13 A Schematic of the ADSA-P experimental set-up. It shows an example of pendant drop surface tension measurements. (Reference: www.ipfdd.de/research/ res12/adsa_p.html)

ADSA-P is based on the comparison of the experimentally observed drop shape with a theoretical formation given by solution of the Laplace equation of capillarity followed by

numerical analysis to estimate surface tension. Two surface parameters, contact angle and surface tension, can be directly measured from a sessile drop or pendant drop, respectively. A schematic of the experimental setup of ADSA-P is shown in Figure 2-13. The sample drop is formed at the end of the motor driven syringe. The drop is then illuminated by a light source to form a clear image on the monitor. The image is amplified through an optical microscope, captured and digitized by a CCD camera, and transferred to a computer, where the image can be analyzed to yield the surface tension of the drop[82].

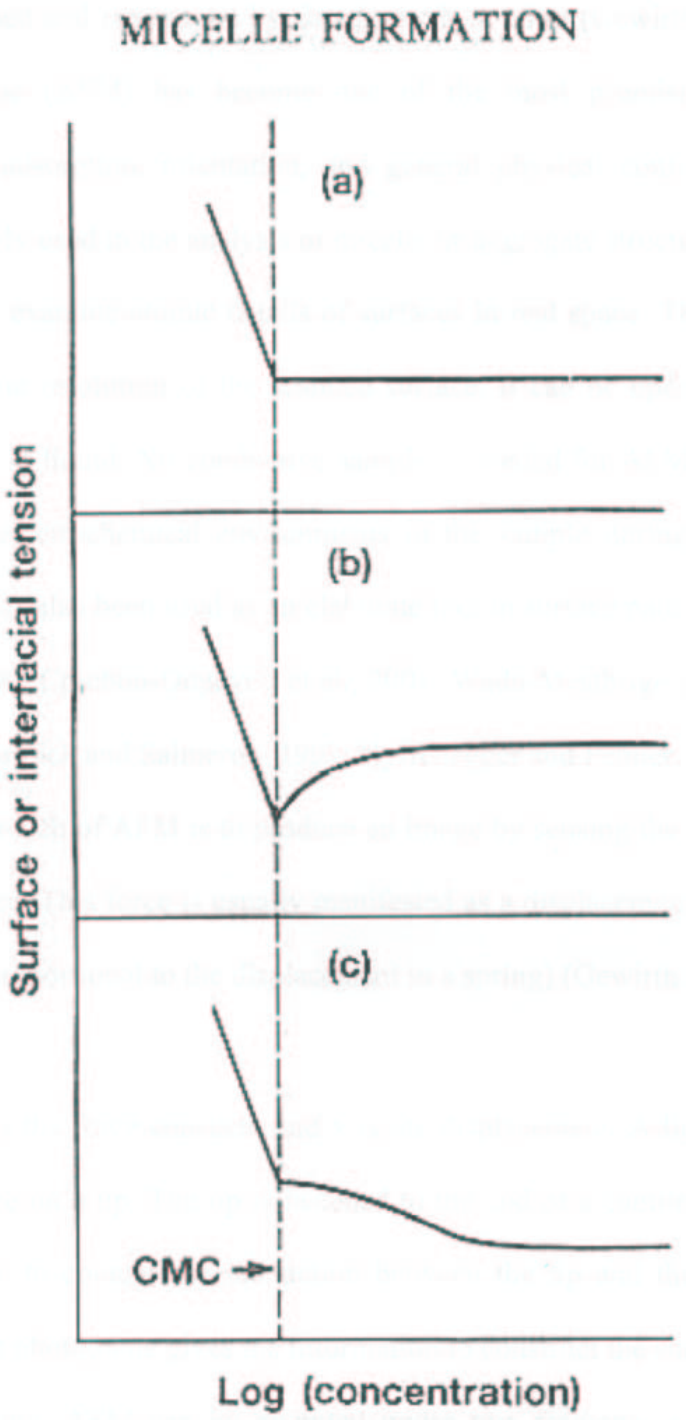

Figure 2-14 Determination of critical micelle concentration from surface or interfacial tension data[74]. (a) shape of curve for pure surfactant; (b) the impurity lowers the surface tension more than the main surfactant; (c) the impurity lowers the tension less than the main surfactant.

Typical results of surface tension measurements for a pure surfactant are shown in Figure 2-14a and indicate that the break point at the CMC can be very sharp and well defined. However, the presence of impurities in the surfactant usually will change the trend of the surface tension curve. The existence of a minimum indicates that an impurity in the surfactant is more surface active than the main surfactant (Figure 2-14b). A less surface-active impurity, on the other hand, will cause a higher break point (Figure 2-14c). One can estimate the CMC from these plots. However, the 'real' CMC cannot be found especially when the plot has a depression or a higher break point. Regardless of this inaccuracy, surface tension is still the most convenient and widely used method for CMC determination.

The surface tension dip has been a widely observed[85-94]. It is believed that even a small amount of impurities can produce this anomaly. It has been proposed that the system must include a small but surface-active and easily solubilize component(s) (the impurity). At concentrations smaller than the CMC the impurity lowers the surface tension below that of the pure surfactant because of its high surface activity. Together, the impurity and the surfactant form mixed micelles. These mixed micelles appear at lower concentrations than those of the pure surfactant. The impurity is depleted in the solution and in the surface by the mixed micelle formations because it is ready solubilized by the micelles. The surface tension is thus raised effectively to the value of the pure surfactant.

2.10.2 Atomic Force Microscopy

AFM, belonging to the family of scanning probe microscopy, generates images by the "feel" rather than the appearance of a specimen. It has the potential to achieve molecular or even sub-molecular resolution. The ability to obtain image under natural conditions is appealing to biologists. Light microscopes are limited by a resolution of 200 nm[95]. AFM images are obtained by measuring changes in the magnitude of the interactions between the probe and the specimen surface as the surface is scanned beneath the probe. Hence, resolution depends on how the interactions vary with separation difference. For macromolecules, atomic resolution is only possible for simple molecules in which each atom is in intimate contact with the surface of a flat substrate.

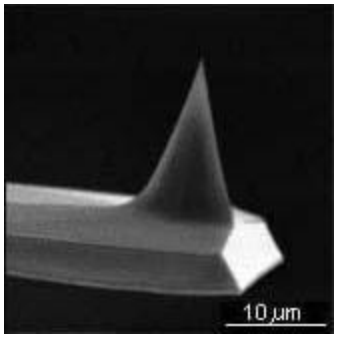

Figure 2-15 Atomic Force Microscope (AFM) tip.

(Reference: http://www.chem.utoronto.ca/staff/MCG/sc12_3.jpg)

AFM is different from a conventional microscopy in that it no optical lenses of any kind is used. The tip consists of an extremely sharp microfabricated spike mounted to the end of a cantilever (Figure 2-15). The sharpness of the spike determines the resolving power of the instrument. The cantilever allows it to move up and down as it tracks the sample similar to a stylus over a record. The cantilever usually has a low spring constant enabling the AFM to control the force between the tip and sample with precision. Cantilever-tip assembly is generally

made of silicon or silicon nitride, these materials being both hard (wear resistant) and ideally suited for micro fabrication.

The tip is moved relative to the sample surface by means of a piezoelectric transducer (Figure 2-16). When a crystal of piezoelectric ceramic is squeezed, it produces a potential difference (bias voltage) large enough to generate a spark. The piezoelectric ceramic can be made to move with an accuracy on the order of the atomic scale. The sample is mounted on top of the piezoelectric transducer.

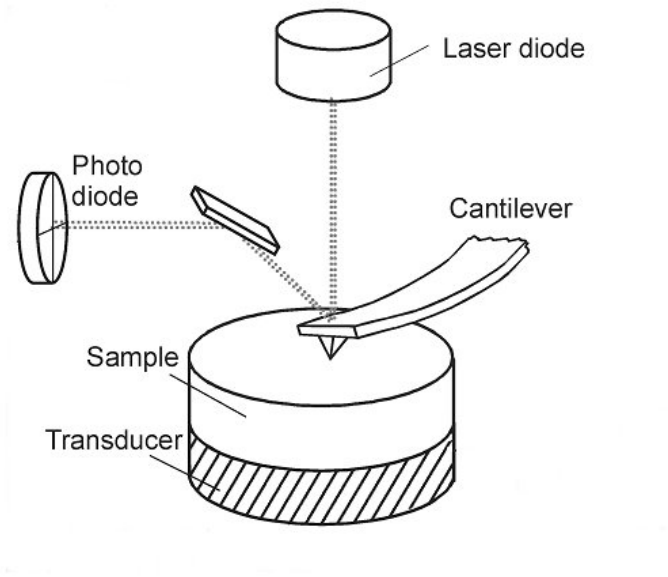

Figure 2-16 Schematic of a typical atomic force microscope

(Reference: http://www.soest.hawaii.edu/~zinin/images/afm.jpg)

The motion of the tip is monitored as it moves across the sample. A laser beam is focused onto the end of the cantilever then reflected off onto a photodiode detector. This mechanical amplifier is sensitive enough to detect atomic scale movement of the tip.

When the sample is scanned, the topography of the sample surface causes the cantilever to deflect as the force between the tip and sample surface changes. The cantilever deflection is maintained at a constant predefined level by a control loop which moves the sample or tip in the appropriate direction at each imaging point.

The AFM can be used to image many types of materials. An AFM can image samples dry or within a wet environment. The liquid cell allows samples to be imaged without the effect of the thin liquid film of air-exposed samples. In contact mode, scanning under ambient air conditions influences the cantilever and tip. Most surfaces are covered by a thin layer of adsorbed gases (typically several nanometers thick), usually condensed water. Once the tip and thin film layer interact, capillary action causes a meniscus to form and surface tension pulls the cantilever down, see Figure 2-17.

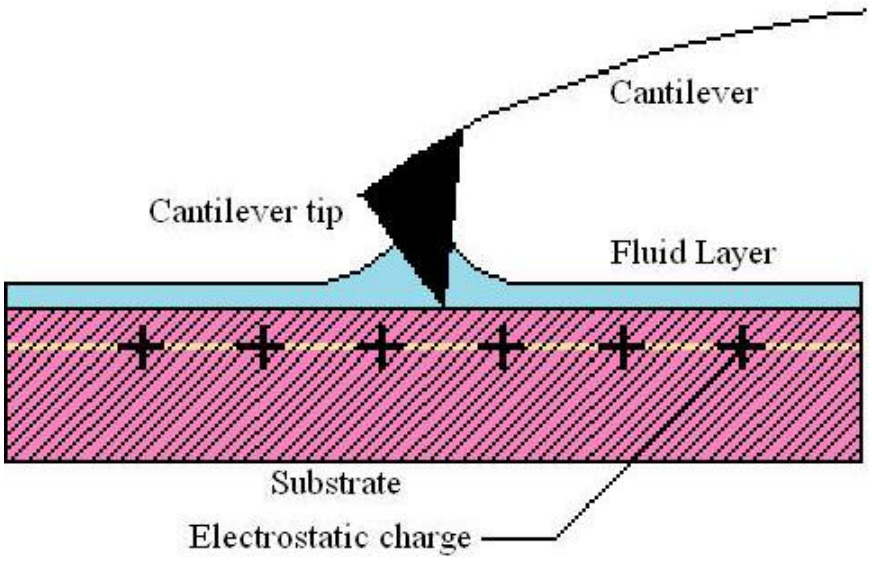

Figure 2-17 Thin film effects on the cantilever of the AFM. The fluid layer on the surface of the substrate interacts with the tip of the AFM and holds it down by surface tension.

This can cause false engagements with the surface, which then can set up a false force set point and in tapping mode will not allow the tip to properly vibrate because it is stuck to the film. It is therefore important to maintain a low humidity environment for scanning.

For hard surfaces the force applied to the surface can be quite high and so the thin film effects can be overcome, but for soft samples, especially biological samples, high force set-points can affect the image that is seen. If too light a force is applied, the effects of the thin film on the surface of the sample take over, if too much force is applied, then the sample is deformed by the tip and a false image is taken of the sample. Since a drying process adversely effects most biological samples and sometimes causes them to become sticky and impossible to image, it is favorable to use the liquid cell. This allows a minimal force to be applied for accurate imaging of the sample.

There are many different types of cantilevers available for various types of imaging and imaging conditions. For hard surface, a stiff cantilever, with a high spring constant can be used for high resolution. A stiff cantilever ensures that the tip is in contact with surface virtually the entire time and will interact with every molecule on the surface. This would not work for a soft biological sample, as it would deform the surface. Thus highly flexible cantilevers with low spring constants are used for biological samples so that more force can be applied to the surface without sacrificing tip response to surface changes. As well, when imaging in the liquid cell in tapping mode, the flexible cantilevers allow for a lower frequency to be used, which reduces the noise caused by the vibrations of the solution, which are caused by the vibration of the cantilever. By using tapping mode, the effect of the tip sticking to materials such as cells or tissues is reduced and therefore using tapping mode increases the overall image resolution.

2.9.3 Light Scattering

Static and dynamic light scattering are well known technique for the characterization of size, shape, anisotropy, and even aggregation behavior of particles. Particles with sizes ranging form 0.01 to 10 μm, usually microcapsules, can have their sizes measured by light scattering techniques, which are complementary to optical, electron and other forms of microscopy[96].

3.0 EXPERIMENTAL

3.1 Preparation of Peptide Solution

The peptide, EAK16-II with the sequence ACn-AEAEAKAKAEAEAKAK-cNH_2 and molecular weight 1656.79 g/mol was purchased from Invitrogen Corporation (CA, US) in crude and purified forms. Peptides in the crude form have a purity level between 50 wt% and 70 wt%. High purity peptide was purified by HPLC and received at >95% purity level. The peptide was dissolved in deionized water (Millipore, 18.6 Ω) at different concentrations ranging from 0.01 mg/mL to 0.9 mg/mL. The seeding agents, L-amino acid monomers alanine, glutamic acid and lysine were purchased from Sigma Aldrich (ON, CAN). Amino acids were dissolved in deionized water (Millipore, 18.6 Ω) and then combined with the peptide at the desired molar ratio. The solutions were stirred by a Vortex mixer for 2 minutes to ensure the peptides were dissolved. All samples were maintained at room temperature ~23°C. The surface tension, AFM and light scattering measurements were performed 14 days after the sample preparation to allow EAK16-II assemblies to reach equilibrium as mentioned by previous studies[64].

3.2 Surface Tension Measurements

Axisymmetric Drop Shape Analysis–Profile (ADSA-P) was used to measure the dynamic surface tension of EAK16-II solutions. In a dynamic process, the surface tension varies as a function of time. For a typical surfactant, the surface tension decreases with time before reaching an equilibrium value. The experimental setup has been described previously[97]. The sample chamber is saturated with pure water vapor to maintain constant humidity. The pendant drop was formed using a syringe needle (inner diameter, 0.92 mm). The surface tension was obtained as a fitting parameter when the experimental drop profile was fitted to the theoretical curve governed

by the Laplace equation of capillarity. The surface tension was measured over a minimum duration of 4-hours/samples. For each run, images were acquired at 60 s intervals. All surface tension measurements were performed at room temperature.

3.3 Atomic Force Microscopy

The nanostructure of the aggregates was investigated using Atomic Force Microscopy (Digital Instruments, US). Before imaging, 10 µL of the peptide solution was placed onto a freshly cleaved mica surface, which was prepared by cleaving the top surface with scotch tape and affixed to a multiple-use stainless steel AFM sample disk. The sample was left for 10 minutes to allow the peptide to adhere to the mica surface. It was then rinsed three times with 20 µL of pure water. The sample plate was covered with a petri dish and placed in a desiccator to avoid contamination for at least 3hrs to allow complete drying. Silicon Nitrite tips was used for AFM contact mode imaging. All images are displayed as 2x2 μm^2 in dimension.

Special care is given to the preparation of samples for AFM imaging. Allowing the peptide solution to 'dry' on the mica surface can cause the solution to become more concentrated as water evaporates from the surface. This can alter the peptide assembles before they are images by AFM. To avoid this effect, the sample is rinsed so that excess peptide is removed from the surface so that a monolayer will absorb onto the mica. Imaging in liquid cell would be most ideal and would eliminate this process. However, the resolution of liquid cell is limited compared to imaging in air and tip fouling becomes an issue. Alternatively, tapping mode in air is ideal for soft biological samples such as tissue or cells. In this study contact mode was selected since the dried peptide monolayer on mica can be considered a hard surface and imaged with higher resolution than liquid cell or tapping modes.

3.4 Light Scattering

The light scattering experiments were carried out using a steady-state fluorescence system (type LS-100, Photon Technology International, ON, CAN) with a pulsed xenon flash lamp as the light source. A right-angled cuvette was used to hold the sample solutions, and the scattered light was monitored at 90 degree from the direction of the incident light. The samples were irradiated using incident light with wavelength 314 nm and the scattered light was monitored in the wavelength range of 300 nm to 325 nm. The peak in the wavelength region arises from the interaction of the EAK16-II aggregate and the incoming excitation light.

The excitation and emission slit widths of the monochromators, which controls the amount of light entering and leaving the sample chamber, were set to 1 nm and 4 nm, respectively. The intensity of the emitted fluorescence was monitored for each sample. These intensities were normalized by the emission intensity obtained for a blank solution containing deionized water to account for day-to-day variations in equipment performance. Blank solutions were tested prior to each peptide solution.

4.0 RESULTS

4.1 High Purity and Crude Peptide

Both high purity and crude forms of the EAK16-II peptide were used in these experiments. The crude peptide has an estimated purity of 50-70 wt%. The HPLC-treated peptide has purity level of 95 wt%. The peptides readily assemble to form nano- and even macrostructures in solution that are concentration dependant. It has been suggested that the addition of salt can induce macrostructure formation[98]. For the purpose of comparing the crude and pure forms of EA16-II no salts or additives were used. The crude peptide batch used in these experiments was estimated to be of 65% purity. However, uncertainty in this estimation makes it difficult to compare the actual amount of peptide in an EAK16-II solution. Thus, the concentration of the crude peptide in solution includes the EAK16-II peptide as well as impurities.

Light scattering experiments were used previously to determine the growth of aggregates with time[64]. The difference in light scattering of the crude and high purity EAK16-II peptide is shown in Figure 4-1. Intensities were measured after peptide was immersed and allowed to reach equilibrium. This occurred after a 14-day period, when no further increases in light scattering was observed, and normalized by a water standard. The crude peptide shows higher light scattering than the high purity peptide at concentrations above 0.09 mg/mL. However, below this concentration, no significant difference in the light scattering is evident. At concentrations greater that 0.3 mg/mL, a thin gel coating on the walls of the glass vial is noticed for both high purity and crude peptide samples. This may contribute to the decrease in the light scattering at the 0.6 and 0.9 mg/mL concentrations from the expected trend.

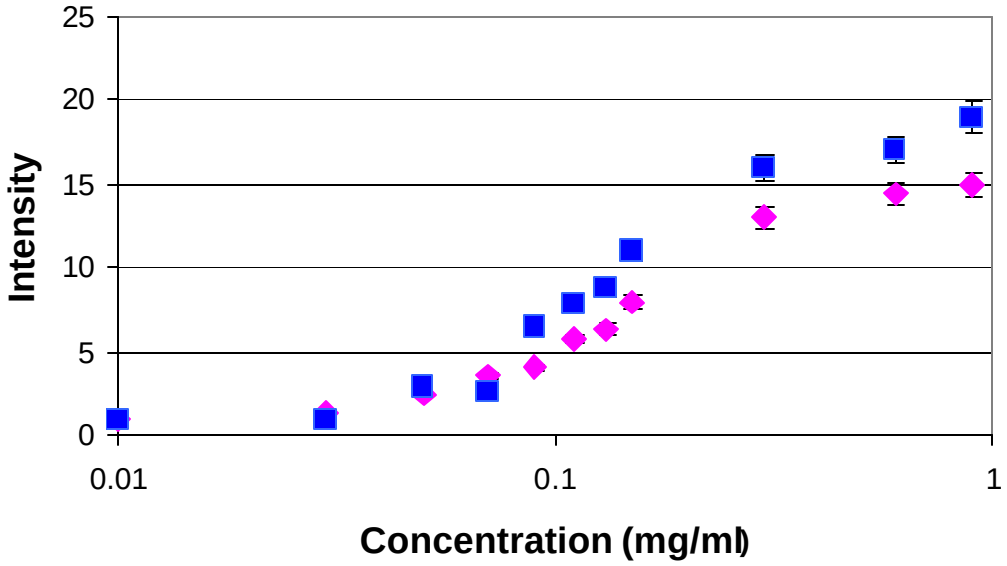

Figure 4-1 Light scattering intensities of 95% pure (diamonds) and crude (square) EAK16-II peptide solutions as a function of peptide concentrations. Intensities averaged after a 14-day period and normalized by water standard.

The dynamic surface tension was measured for each peptide sample over a four-hour period. These surface tension-time profiles are characterized by an induction period followed by an exponential drop until equilibrium is reached[74]. To obtain the 'equilibrium' surface tension from the dynamic surface tension date, an extrapolation method is used[99]. For each concentration, the surface tension is plotted versus $1/t^{0.5}$. The equilibrium surface tension is estimated by a linear extrapolation of $1/t^{0.5}$ to the y-axis (i.e. $t \to \infty$). This plot is based on the assumption that the surface adsorption process occurs according to a diffusion-controlled mechanism. The equilibrium surface tensions obtained by the extrapolation method are plotted as a function of concentration of crude and high purity EAK16-II in Figure 4-2.

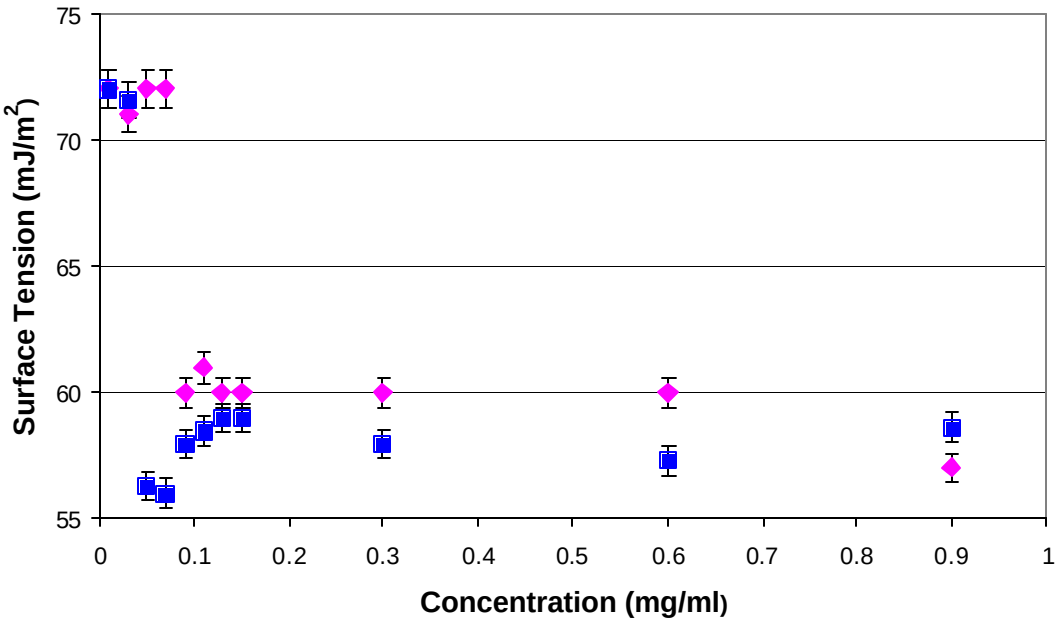

Figure 4-2 Equilibrium surface tension profile of 95% pure (diamonds) and crude (squares) EAK16-II at as a function of peptide concentration. Values indicate the extrapolated equilibrium surface tension values. The critical aggregation concentration is found to be around 0.09 mg/mL in both cases.

The high purity peptide shows an equilibrium surface tension of about 72 mJ/m^2 at low EAK16-II concentrations. This value is close to that of pure water. When the concentration increases, the surface tension drops down to about 60 mJ/m^2 at a peptide concentration of 0.09 mg/mL. This is close to the reported EAK16-II critical aggregation concentration (CAC) of 0.1 mg/mL[64]. At higher concentrations the equilibrium surface tension remains relatively constant at approximately 60 mJ/m^2. Although it does drop below this value at high enough concentrations.

Nevertheless, no surface tension 'dip' was observed for the high purity peptide. Instead, a very sharp break point is observed at the CAC.

The crude peptide also shows an equilibrium surface tension of 72 mJ/m^2 at low EAK16-II concentrations. However, the surface tension drops dramatically to 56 mJ/m^2 at low peptide concentrations of 0.05 and 0.07 mg/mL, then increases back to about 58 mJ/m^2 at higher concentrations. The small 'dip' in the curve appears to be due to the presence of impurities in the crude peptide. It has been reported that, depending on their surface activity, the impurities may cause either a minimum or a higher break point in the surface tension-peptide concentration plot[74].

Atomic Force Microscopy (AFM) was used to obtain images of the morphology of the peptide aggregates. The differences in the peptide morphology are apparent upon the onset of fibres. In the high purity peptide samples, fibre formation begins at 0.09 mg/mL concentrations. Below this concentration the peptide takes the form of globular aggregates (Figure 4-3a). However, for the crude peptide, some fibre formation is seen to begin at concentrations as low as 0.05 mg/mL (Figure 4-4a). This indicates that the presence of impurities may be responsible for the formation of fibre below the CAC. Above the CAC, fiber formations are observed for both the crude and high purity peptide (Figure 4-3b and 4-4b).

A B

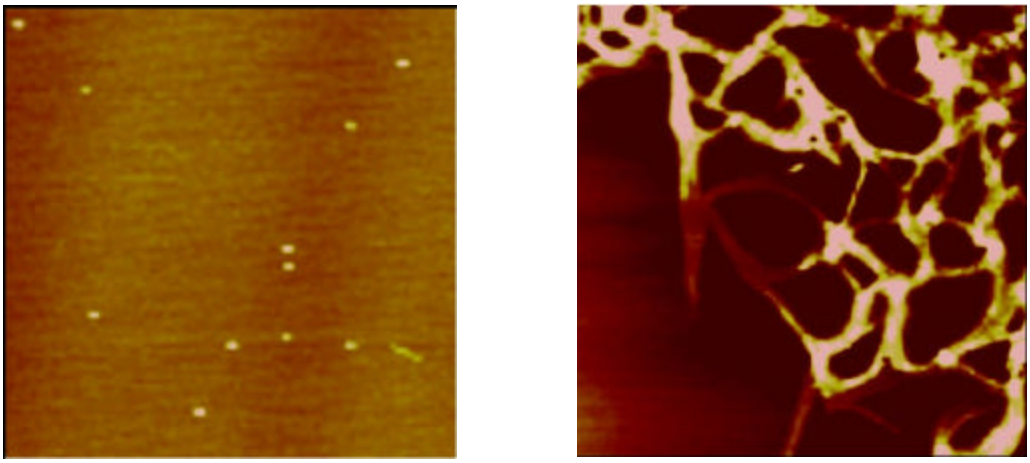

Figure 4-3 AFM images of high purity (<95wt%) EAK16-II morphologies above and below the CAC. (a) 0.07 mg/mL (b) 0.11 mg/mL. Images displayed with 2x2μm^2 dimension.

A B

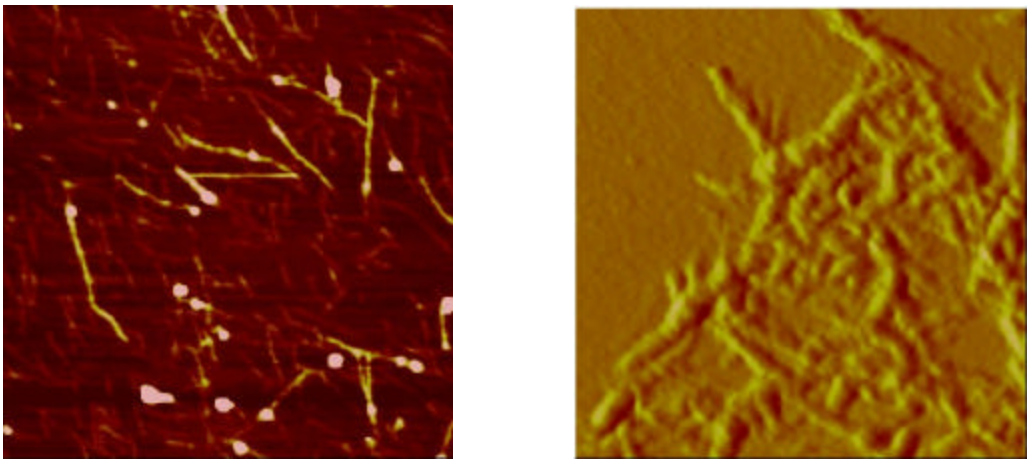

Figure 4-4 AFM images of crude (~65wt%) EAK16-II morphologies above and below the CAC. (a) 0.07 mg/mL (b) 0.11 mg/mL. Images displayed with 2x2μm^2 dimension.

4.2 Seeding Agents

Alanine, glutamic acid, and lysine are the amino acid components of the EAK16-II peptide. Their surface activity is similar to that of water at the concentrations used in these experiments even when monitored over an eight-hour period. The 'seeds', namely alanine, glutamic acid, and lysine are not surface-active at the concentrations used in this study as shown in Figure 4-5.

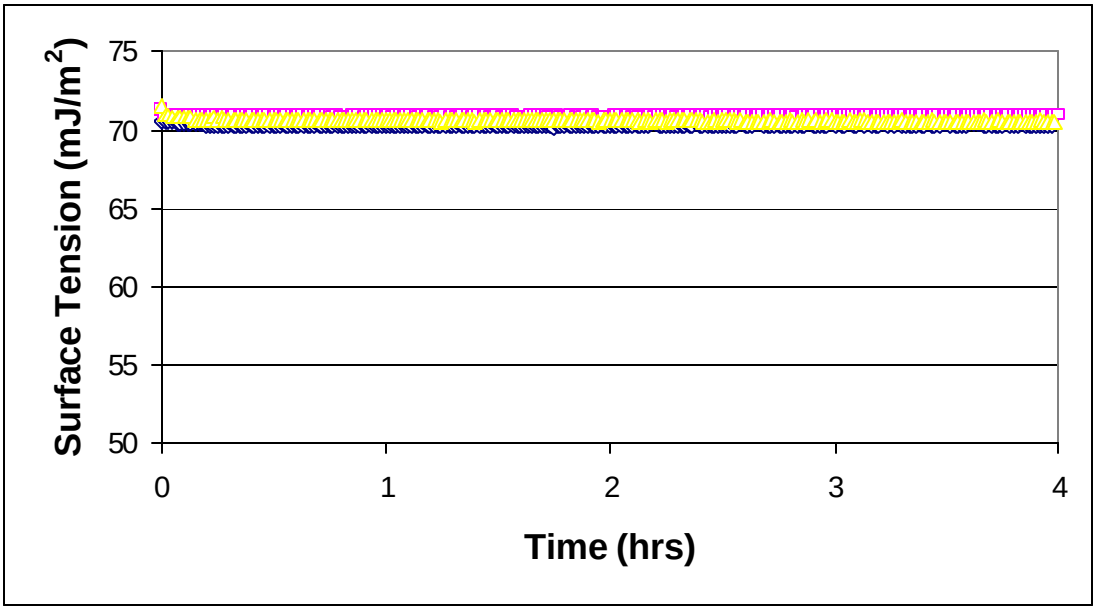

Figure 4-5 Surface tension-time profile of amino acid monomers alanine, glutamic acid, and lysine.

4.3.0 Alanine

High purity peptide was seeded with alanine at various molar ratios. The peptide concentration of 0.07 mg/mL was selected since it coincides with the surface tension 'dip' observed for the crude peptide shown in Figure 4-2. The peptide concentration was held fixed at

this level in all cases as the alanine:peptide ratio was varied (1:50, 1:10, 1:1, 10:1, 50:1, 100:1, 1000:1).

Equilibrium surface tension values were obtained for peptide solutions with varying alanine ratios using the extrapolation method (Figure 4-6). The equilibrium surface tension decreases to a value of 60 mJ/m^2 as the molar ratio of alanine to peptide is increased to 10:1. This value is still higher than the surface tension of 56 mJ/m^2 observed for the crude peptide alone at a concentration of 0.07 mg/mL. At higher molar ratios the surface tension begins to increase. This may be attributed to a reduction in the relative amount of peptide in solution. Since alanine itself is not surface-active at these concentrations, the alanine-rich solutions should be less surface-active.

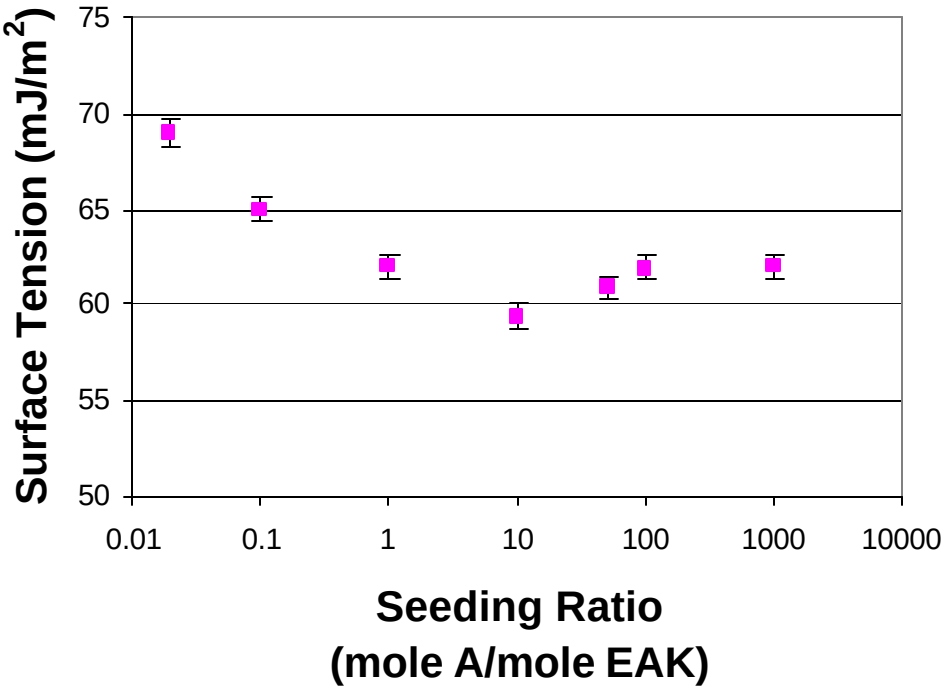

Figure 4-6: Equilibrium surface tension of 0.07 mg/mL EAK16-II solutions (95% pure) as a function of molar ratio of alanine to EAK.

For surface-active biomolecules, an induction time usually occurs under some conditions during dynamic surface tension measurements. The surface tension will change significantly only after this induction period. This is because a certain number of molecules must adsorb at the surface to affect the surface tension. The induction time is also related to the size and amphiphilicity of the species in solution. Figure 4-7 shows that the induction period decreases as the molar ratio of the seeding agent to peptide approaches 10:1. At higher ratios, the induction period begins to increase.

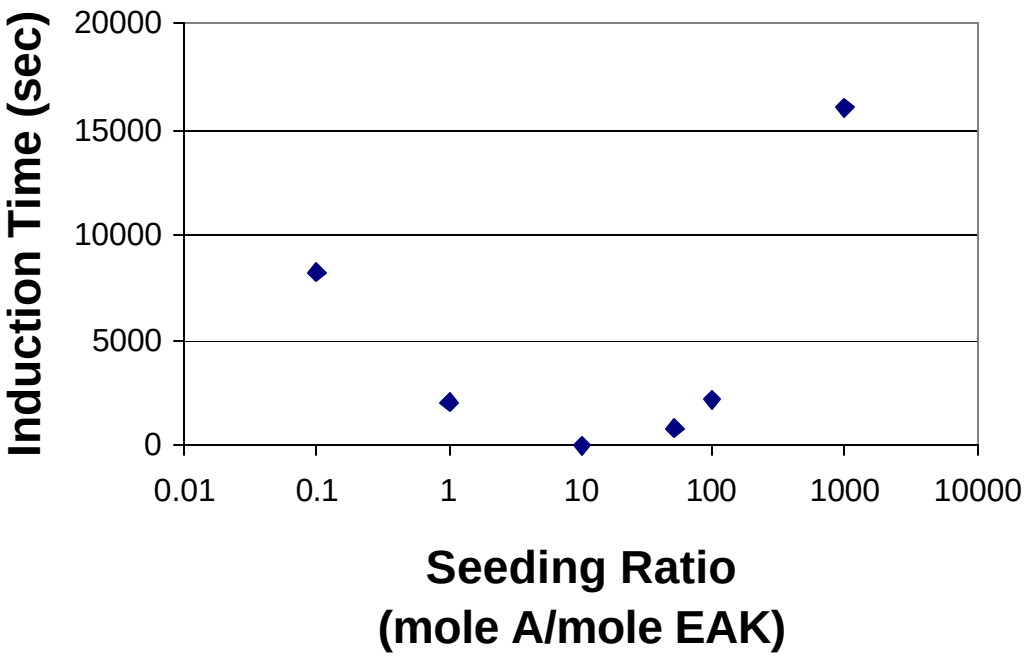

Figure 4-7 Induction time of 0.07 mg/mL high purity EAK16-II as a function of molar ratios of alanine to EAK16.

The morphology of the nanostructures has been observed by atomic force microscopy. As the molar ratio of alanine is increased, the amount of fibre formation appears to reach a

maximum at a 10:1 ratio. At higher alanine concentrations, the amount of peptide assemblies is diminished and fewer fibres are observed, although the fibres appear to be thicker (Figure 4-8). At the high alanine ratio, crystalline structures are observed.

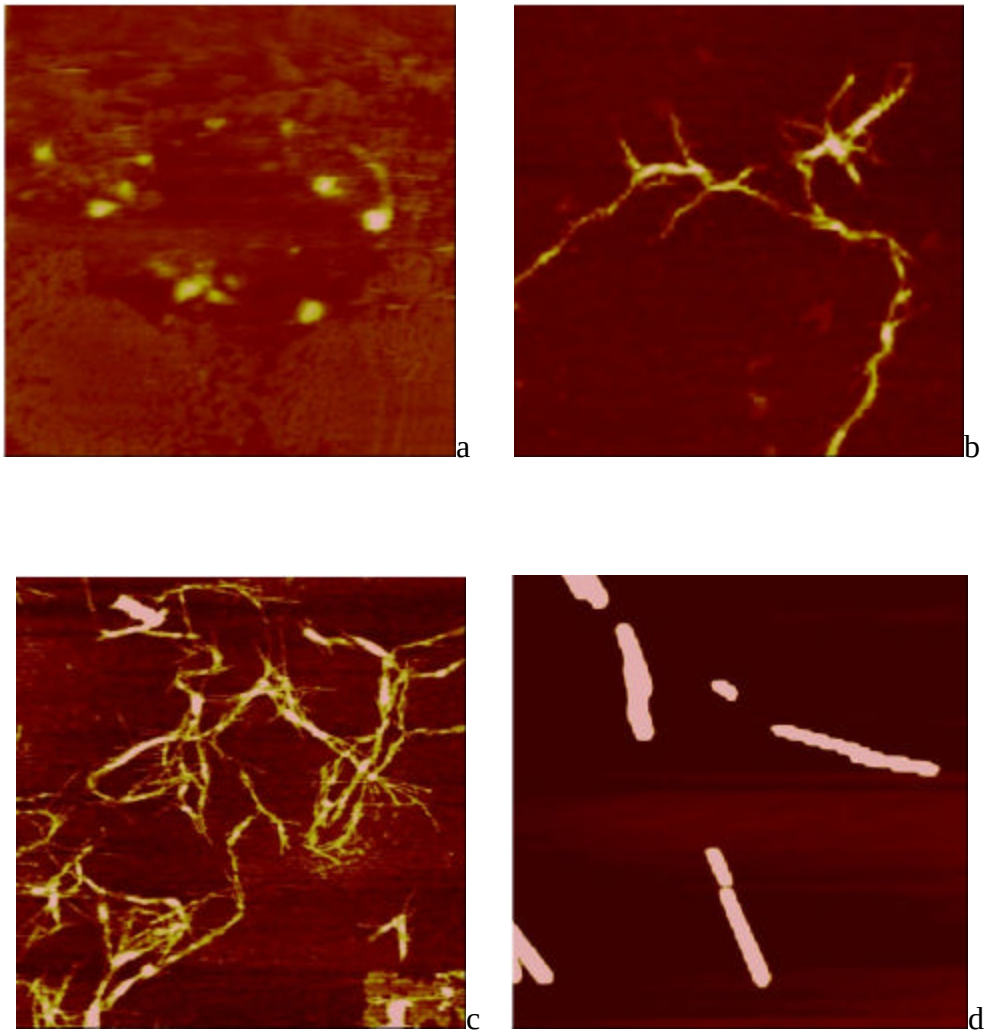

Figure 4-8 AFM images of 0.07 mg/mL high purity peptide with varying alanine ratios: (a) 1:50, (b) 1:1, (c) 10:1, (d) 1000:1. Images displayed with 2x2μm^2 dimension.

4.3.1 Alanine and Peptide Concentrations

A alanine:peptide molar ratio of 10:1 was selected to determine the effect of alanine seeding at various peptide concentrations. The 0.07 mg/mL concentration was originally selected since it coincides with the surface tension dip in the crude peptide samples (Figure 4.2). Peptide concentrations of 0.03, 0.07, 0.11 and 0.3 mg/mL were studied in this series of experiments.

The presence of alanine was observed to cause the surface tension of the peptide to decrease at low concentrations. However, no 'dip' was observed around 0.07 mg/mL but instead appeared to occur between 0.11 and 0.3 mg/mL (Figure 4-9). At the higher concentration, 0.3 mg/mL, the surface tension returned to the expected value for pure peptide, 60 mJ/m^2.

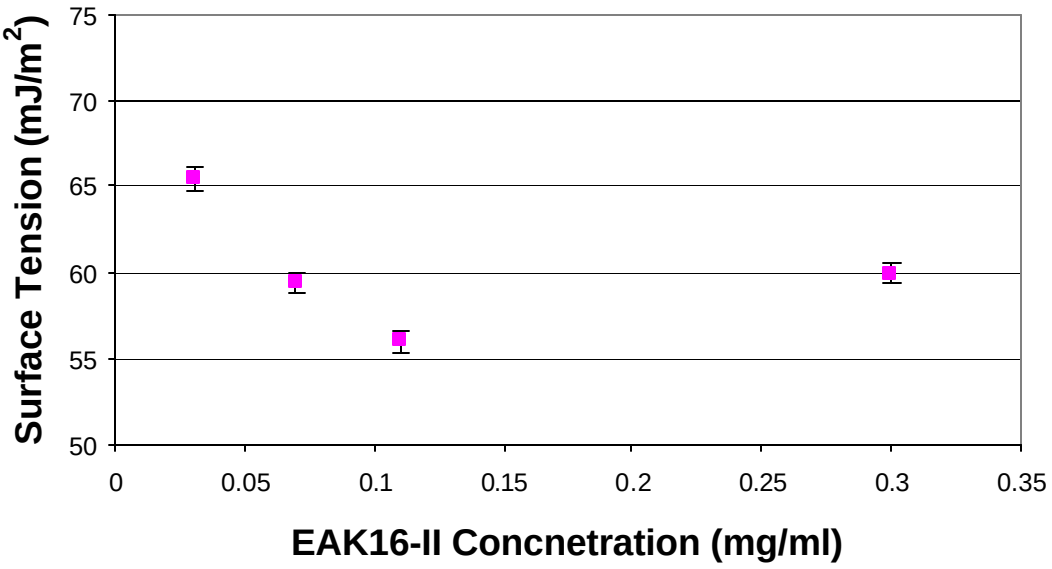

Figure 4-9 Equilibrium surface tension of high purity peptide with 10:1 (A:EAK) mole ratio as a function of peptide concentrations. Peptide concentrations 0.03, 0.07, 0.11 and 0.3 mg/mL were studied.

The surface tension results are well reflected in the peptide morphology observed by AFM. The 10:1 alanine-to-peptide seeding ratio induced fibre formation at low peptide concentrations (Figure 4-10). These fibres appear to have discrete lengths. At higher concentrations, the fibres tend to link together to form networks.

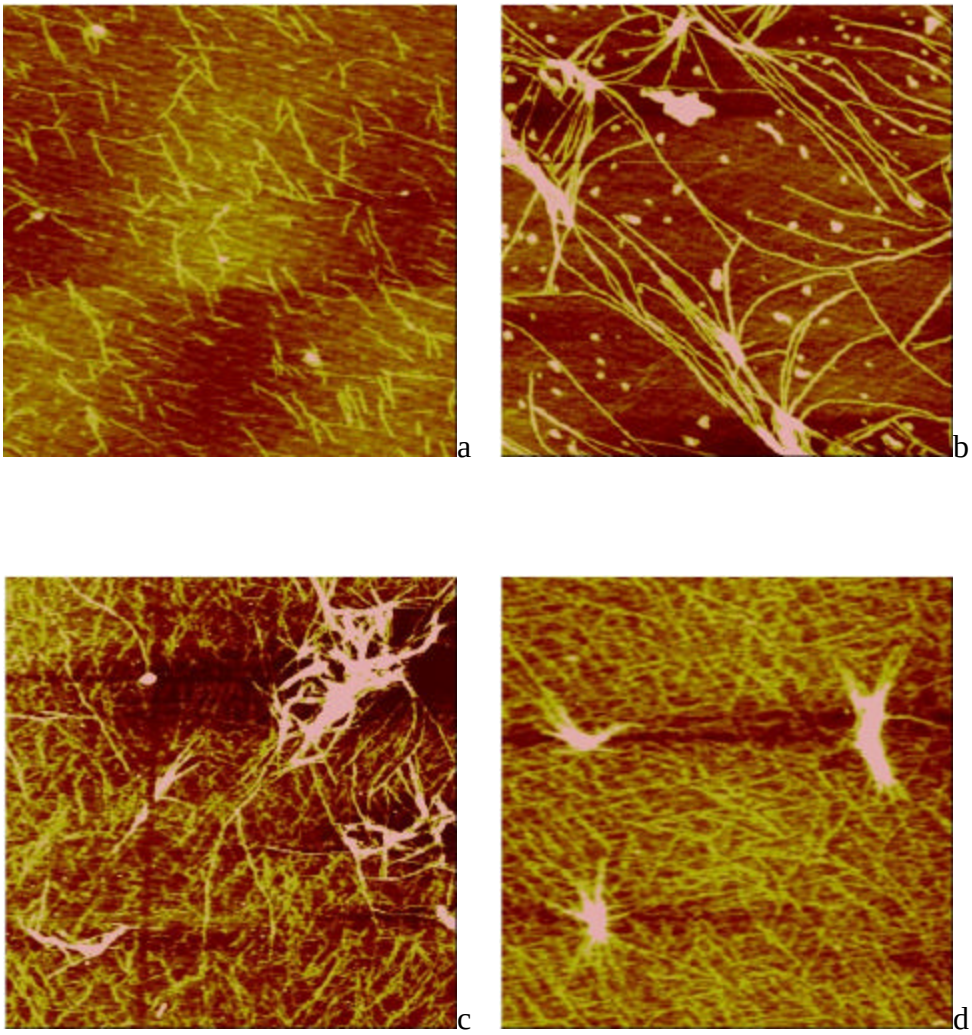

Figure 4-10 AFM images of EAK16-II (95%pure) with 10:1 (A:EAK) mole ratio at (a) 0.03 mg/mL, (b) 0.07mg/mL, (c) 0.11mg/mL and (d) 0.3mg/mL peptide concentrations. Images displayed with $2x2\mu m^2$ dimension.

4.4.0 Glutamic Acid

Glutamic acid, carrying a negative charge at neutral pH, was combined with high purity peptide at various molar ratios. The peptide was maintained at the low concentration of 0.07 mg/mL while the glutamic acid monomer:peptide mole ratio was varied from 1:50, 1:10, 1:1, 10:1, 50:1, 100:1 and 1000:1. The dynamic surface tension was monitored for at least 4 hours in each case. The extrapolation method was used to determine the equilibrium surface tensions (Figure 4-11).

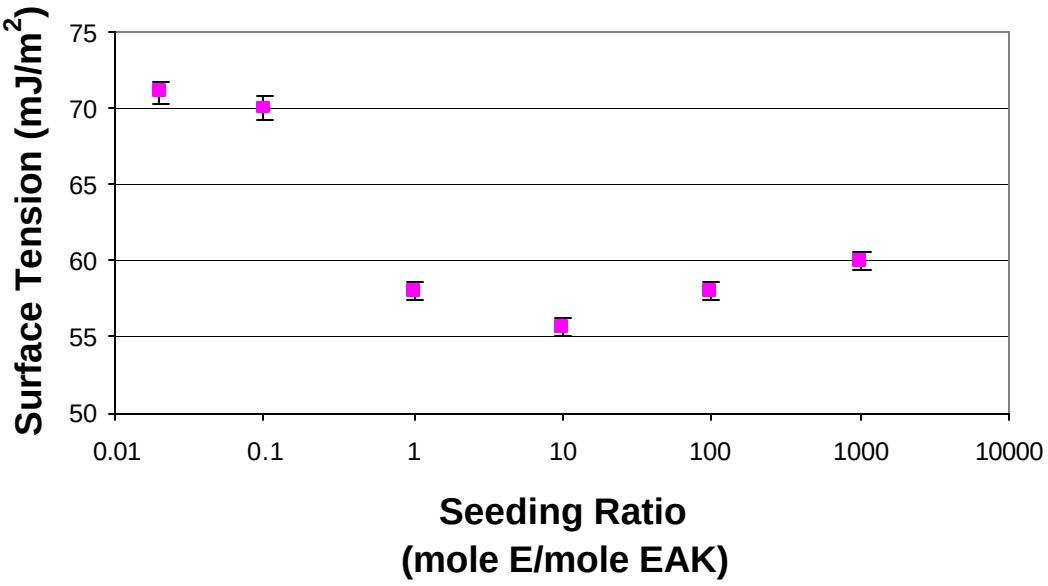

Figure 4-11 Equilibrium surface tension of 0.07mg/mL EAK16-II solutions (95% pure) as a function of molar ratio of glutamic acid to EAK.

The equilibrium surface tension begins to change after the glutamic acid-to-peptide mole ratio reaches 1:10. A minimum equilibrium surface tension value of about 55 mJ/m^2 is observed at a 10:1 ratio. This is the same ratio at which a surface tension minimum was observed for

alanine (Figure 4-6 on page 42). At higher concentrations the surface tension begins to increase slowly.

The induction times for the peptide solution with varying glutamic acid ratios are shown in Figure 4-12. At a seeding ratio below 1:1 the surface tension was similar to that of pure water as no change in the surface tension profile was observes, hence an induction time could not be obtained. The solution with the glutamic acid to monomer ratio of 10:1 exhibited the shortest induction time (Figure 4-12). At higher ratios, more time is required for the peptide to modify the air-water interface.

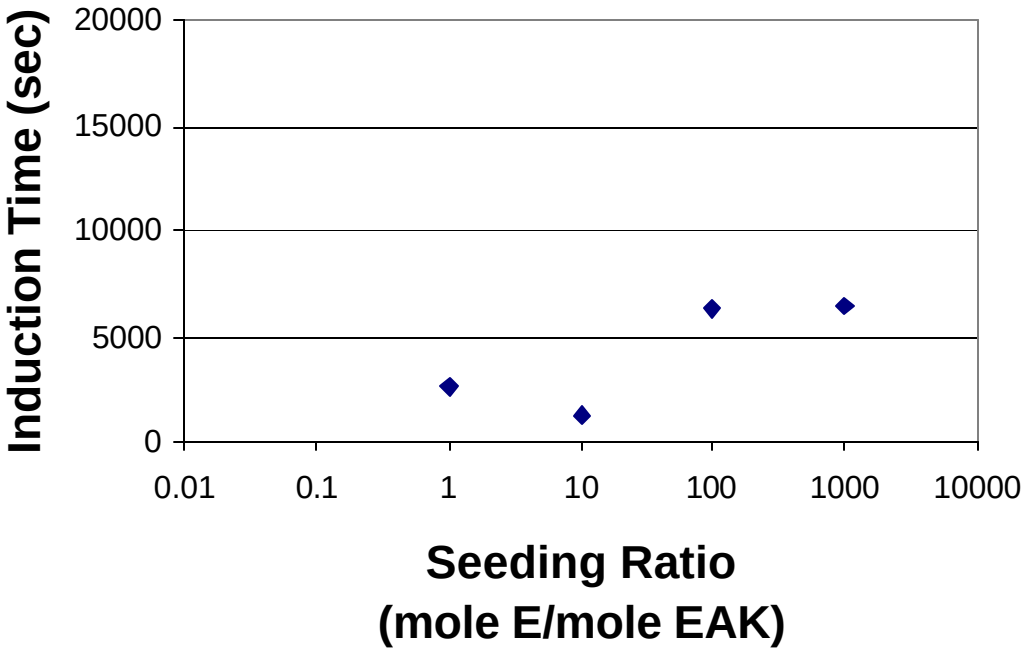

Figure 4-12 Induction time of 0.07mg/mL high purity EAK16-II as a function of molar ratios of glutamic acid to EAK.

The morphologies of the structure formed in the presence of peptide and glutamic acid show fibre formations at all seeding ratios as shown in Figure 2-13. At the high seeding ratio, tree-like crystalline structures are observed.

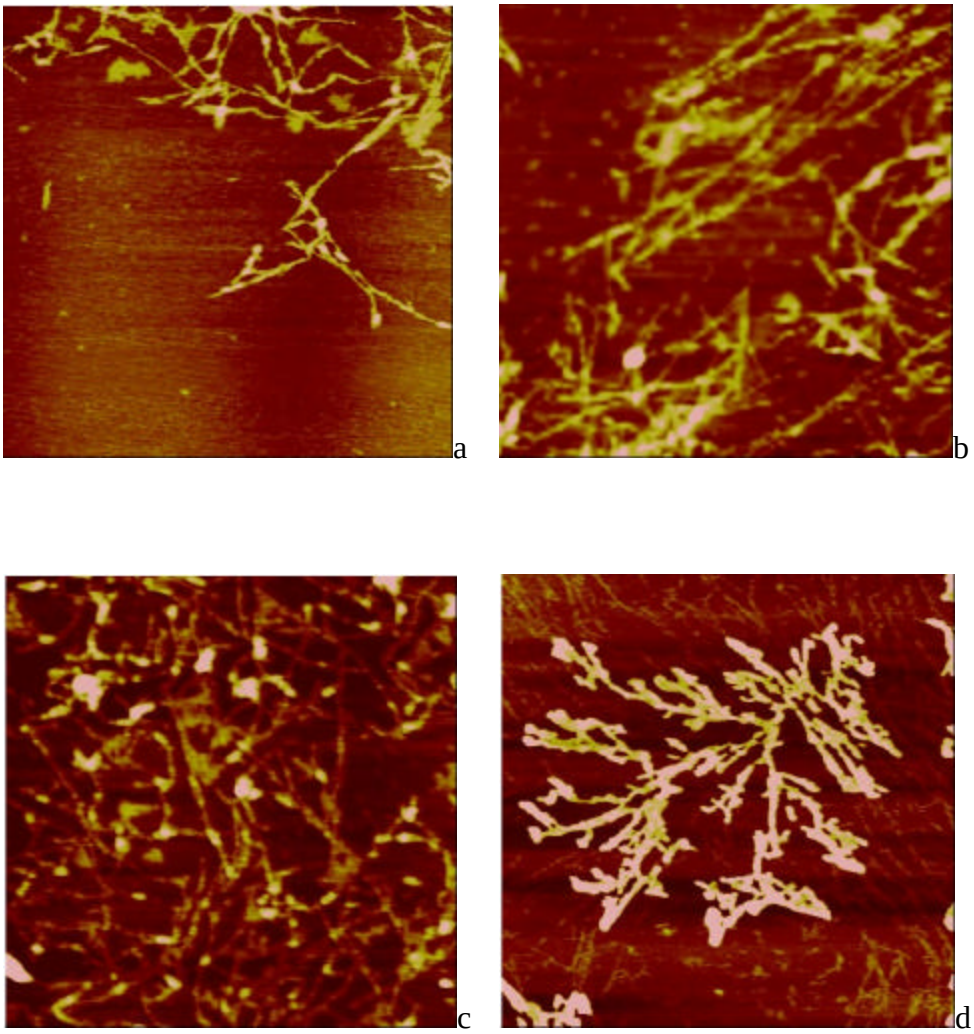

Figure 4-13 AFM images of 0.07mg/mL high purity peptide with varying glutamic acid ratios: (a) 1:50, (b) 1:1, (c) 10:1, (d) 1000:1. Images displayed with 2x2μm^2 dimension.

4.4.1 Glutamic Acid and Peptide Concentrations

The effect of the 10:1 glutamic acid to peptide seeding ratio on peptide concentration around the 0.07 mg/mL concentration was studied. This seeding ratio decreased the surface tension to 65 mJ/m^2 at a low peptide concentration of 0.03 mg/mL (Figure 4-14). The surface tension dips to a minimum of 55.5 mJ/m^2 at 0.07 mg/mL EAK16-II. A similar 'dip' was also observed in the crude peptide (Figure 4-2). The surface tension then rises to about 63.5 mJ/m^2 at higher peptide concentrations.

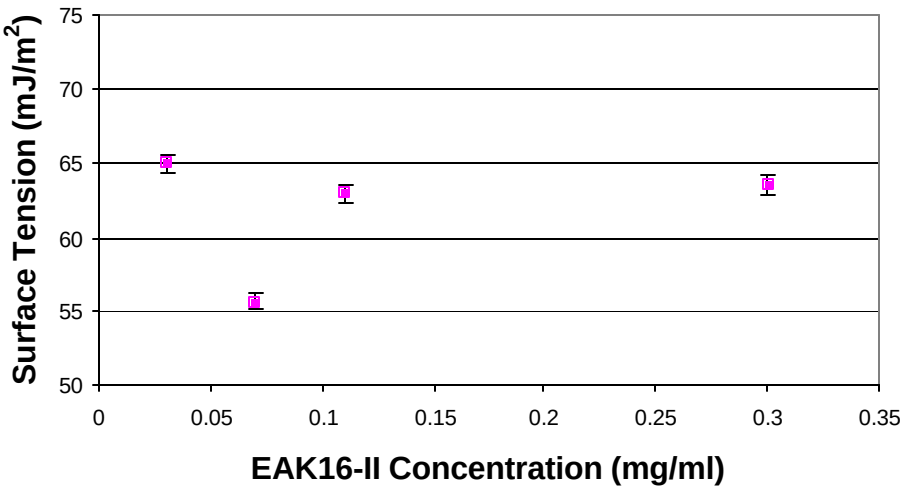

Figure 4-14 Equilibrium surface tension of high purity peptide with 10:1 (E:EAK) mole ratio as a function of peptide concentrations.

The morphologies of the glutamic acid-seeded peptide aggregates all show fibre formation, as seen in Figure 4-15. Fibre formation is observed at all concentrations with the exception of the 0.11 mg/mL concentration, which showed globular structures.

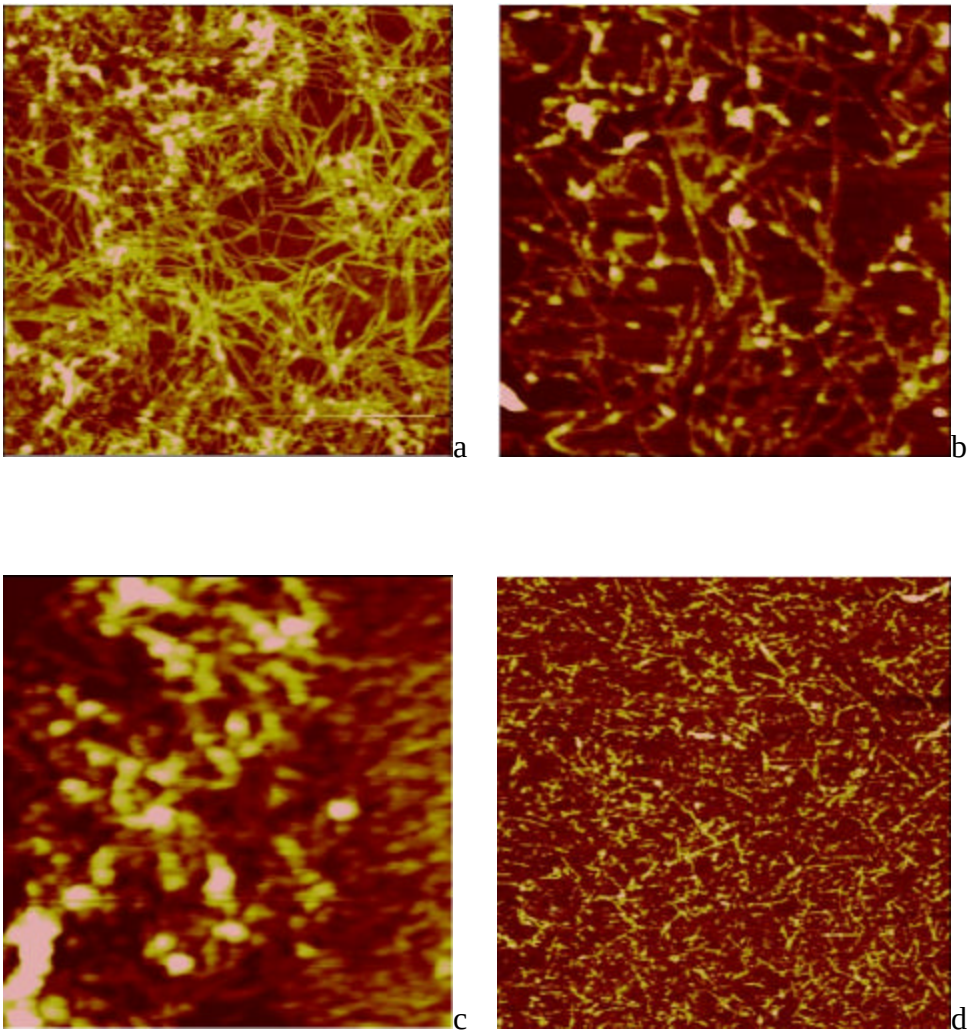

Figure 4-15 AFM images of EAK16-II (95%pure) with 10:1 (E:EAK) mole ratio at (a) 0.03mg/mL, (b) 0.07mg/mL, (c) 0.11mg/mL and (d) 0.3mg/mL peptide concentrations. Images displayed with $2x2\mu m^2$ dimension.

4.5.0 Lysine

The effect of negatively charged lysine on high purity 0.07 mg/mL peptide solution was determined by dynamic surface tension measurements. The equilibrium surface tensions were determined by extrapolation (Figure 4-16). The equilibrium surface tension is similar to that of water (72 mJ/m^2) at a 50:1 molar ratio but decreases to a minimum value of 54 mJ/m^2 at 1:1 molar ratio. The equilibrium surface tension then begins to increase after the 10:1 lysine-to-peptide molar ratio, as has also been observe with alanine and glutamic acid.

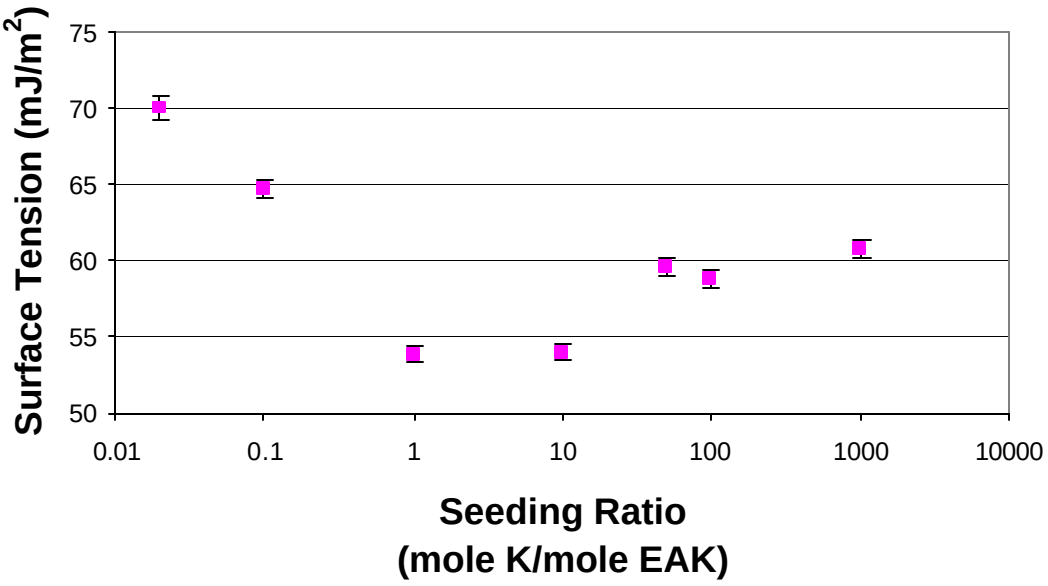

Figure 4-16 Equilibrium surface tension of 0.07mg/mL EAK16-II (95% pure) as a function of molar ratio of lysine to EAK.

The induction periods for the lysine and peptide solutions are shown in Figure 4.17. The induction time for 1:10 mole ratio of lysine-to-peptide is much lower that that observed with either alanine or glutamic acid monomers. At molar ratios above 50-1, the induction time

increases. This may be a result of the dominating effect of the non-surface active lysine in solution.

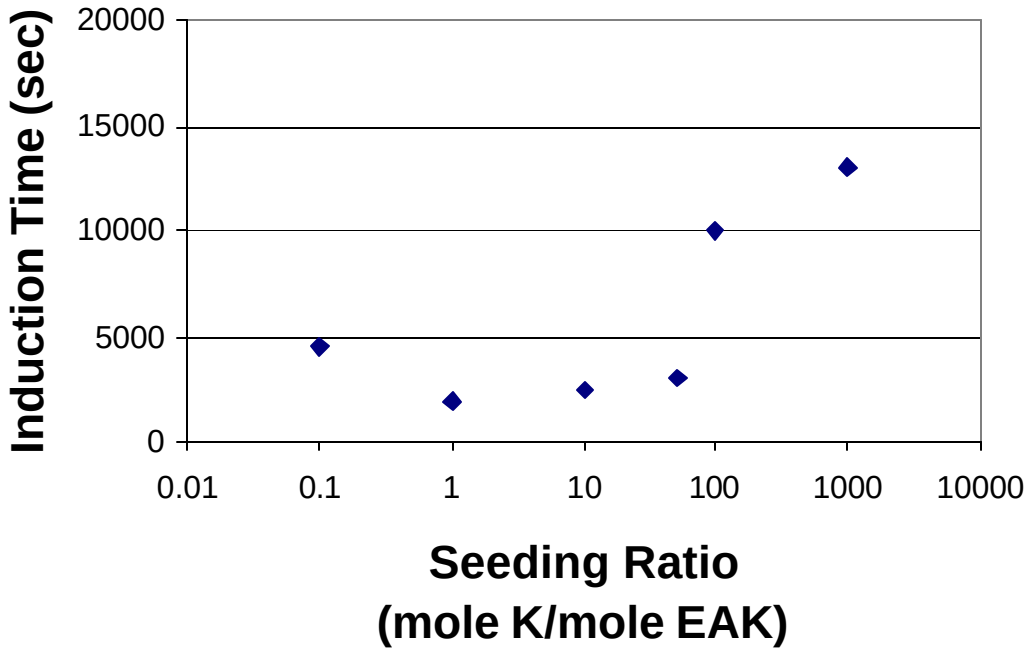

Figure 4-17 Induction time of 0.07mg/mL high purity EAK16-II as a function of molar ratios of lysine to EAK.

The peptide morphologies of the lysine and peptide solutions are shown in Figure 4-18. The formation of fibres appears to correlate well with variations of surface tension with seeding ratio. Fibre formation is observed under conditions where the surface tension and induction times are lowest (i.e., seeding ratios of 1:1 and 10:1).

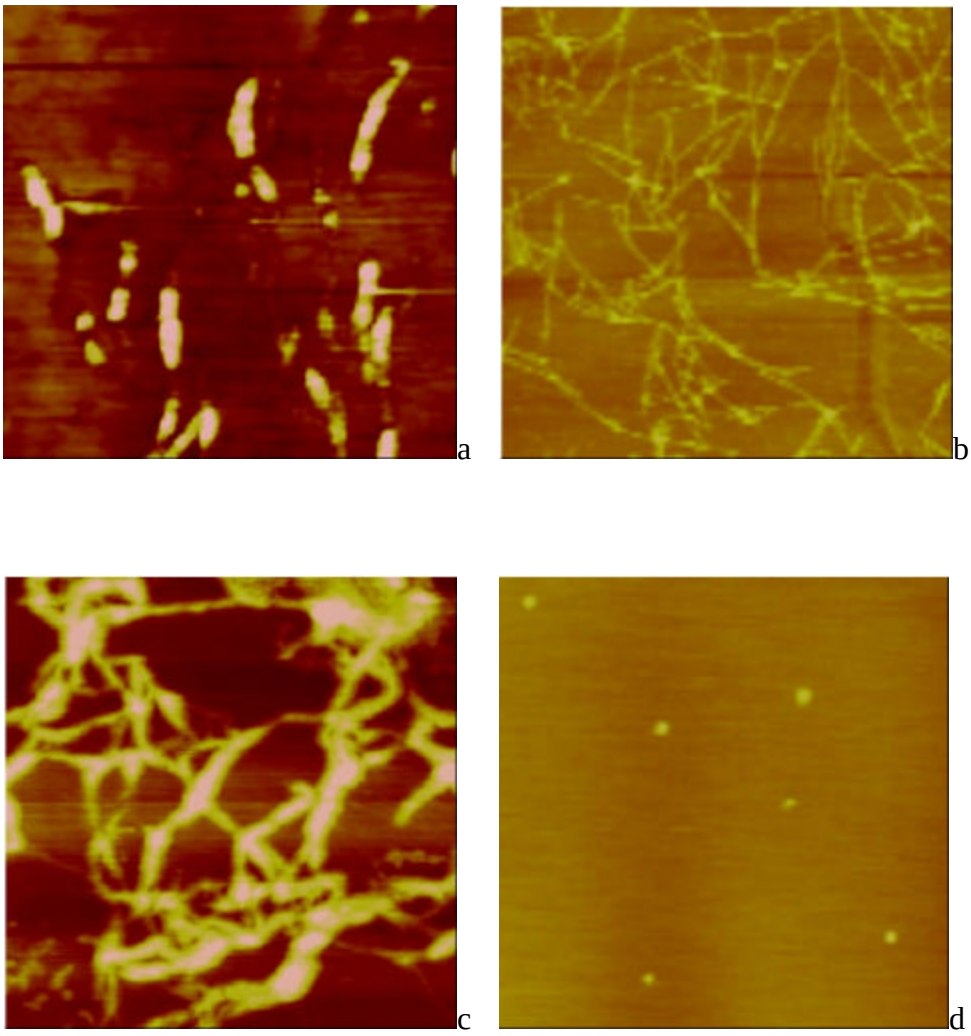

Figure 4-18 AFM images of 0.07mg/mL high purity peptide with varying lysine ratios: (a) 1:50, (b) 1:1, (c) 10:1, (d) 1000:1. Images displayed with $2x2\mu m^2$ dimension.

4.5.1 Lysine and Peptide Concentrations

Again, the effect of peptide concentration at 10:1 lysine:EAK16 mole ratios was determined. The effect of EAK16-II concentrations on equilibrium surface tension was shown in Figure 4-19. The presence of lysine seeding agent decreased the equilibrium surface tension

obtained at 0.03 mg/mL peptide to 62 mJ/m^2. This is much lower than that obtained in the presence of either alanine or glutamic acid at the same ratio (65.1 and 65.2 mJ/m^2). A surface tension 'dip' is observed at the 0.07 mg/mL peptide concentration to a value of 54 mJ/m^2. This is similar to that seen with the crude peptide at the same EAK16-II concentration. At higher concentrations the surface tension increases to 60 mJ/m^2, as seen for pure peptide solutions.

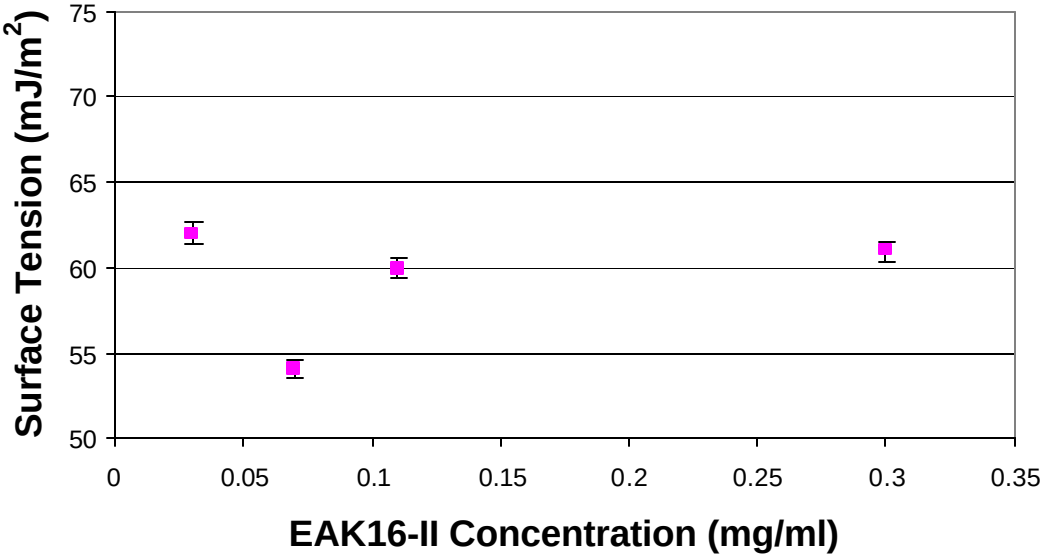

Figure 4-19 Equilibrium surface tension of high purity peptide solutions with 10:1 (K:EAK) mole ratio as a function of EAK16-II concentration.

The morphology of the lysine-peptide aggregates are shown in Figure 4-20. The structures in all cases contain fibres. But they look quite different from one another. At the 0.3 mg/mL concentration the peptide formed a membrane-like structure.

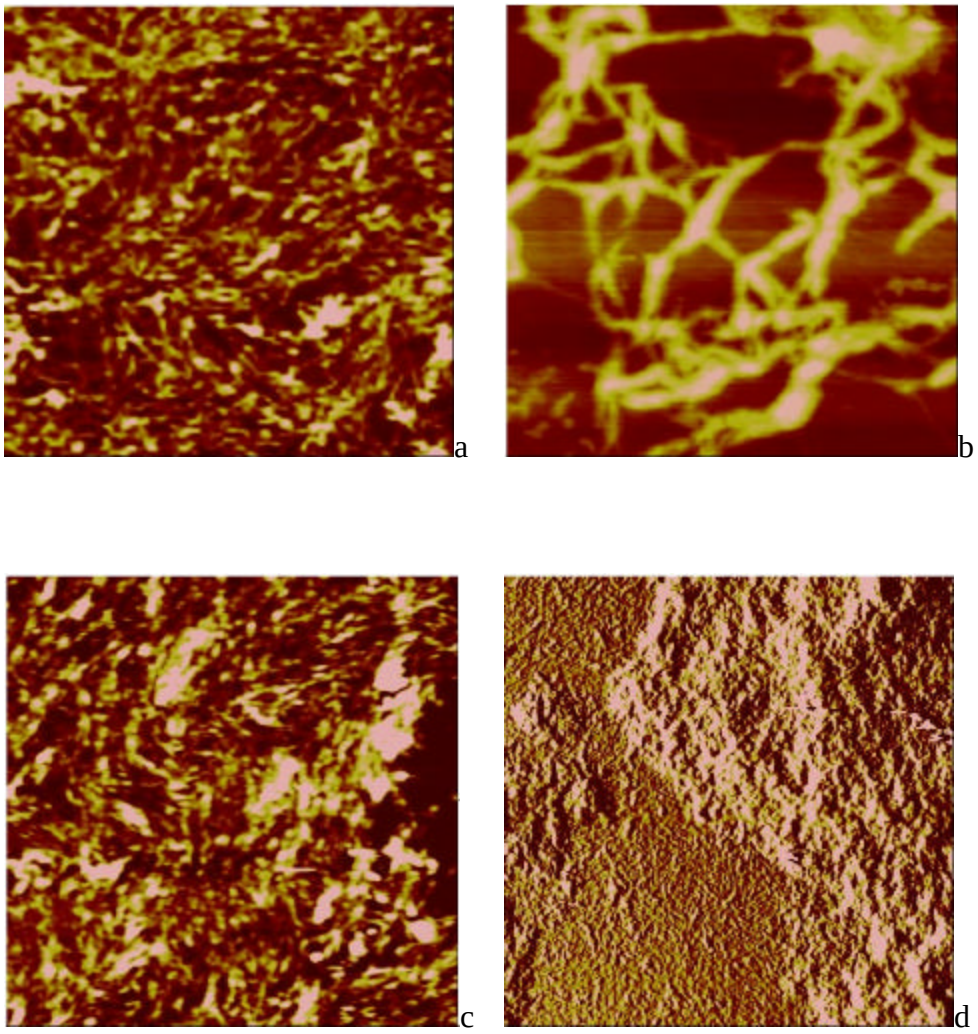

Figure 4-20 AFM images of EAK16-II (95%pure) with 10:1 (K:EAK) mole ratio at (a) 0.03mg/mL, (b) 0.07mg/mL, (c) 0.11mg/mL and (d) 0.3mg/mL peptide concentrations. Images displayed with $2x2\mu m^2$ dimension.

5.0 Discussion

The peptide EAK16-II contains both hydrophobic (alanine) and hydrophilic (glutamic acid and lysine) residues. It forms stable ß-sheets spontaneously in aqueous solutions mainly via hydrogen bonding. Both the electrostatic forces of the charged residues and the hydrophobic interactions contribute to further enhance the aggregation process. This unique amphiphilic structure of EAK16-II is quite different from that of a surfactant, which contains a hydrophobic head and a hydrophobic tail, and thus provides possible explanation of the fibril formation observed. The formation of these assemblies occurs at concentrations above the CAC. However, with the presence of seeding agents these nanostructures can be induced at lower concentrations. Understanding the seeding effect on peptide assembly provides a means to control or direct the formation of desired biomaterials.

The impact of peptide purity of EAK16-II has been examined. The high purity peptide used in this study was HPLC purified to >95% while the purity of the crude peptide was in the range of 50-70%. The crude peptide used in these experiments had a purity level estimated to be 65% with the remaining 35% being composed of truncated or deleted sequences and reagents used in the synthesis process.

Light scattering was performed on both high purity and crude peptide. The light scattering intensity increased with peptide concentration (Figure 4-1). At high concentrations a difference in the light scattering observed in the presence of high purity and crude peptides is apparent at concentrations of 0.09 mg/mL and greater. This is close to the reported CAC value for EAK16-II of 0.1mg/mL[64]. However, at low concentrations, the scattering intensities of both peptide solutions were not significantly different. Since seeding is expected to play a large role at low peptide concentrations, no further light scattering experiments were used in favour of more

sensitive techniques such as surface tension measurements and atomic force microscopy. Nevertheless, the light scatter data does suggest that although the actual amount of peptide in the crude sample is less than the high purity peptide of the same concentration, similar light scatter results can be obtained. This may be attributed to the presence of impurities in the crude sample. This may be beneficial in optimizing the manufacturing nano- or macrostructures with a minimum amount of peptide material

5.1 High Purity Peptide

Surface tension is the measure of the surface activity of a surfactant or its tendency to modify the air-water interface. The critical aggregation concentration for EAK16-II is shown to be 0.09 mg/mL (Figure 4-2). The equilibrium surface tension profile displays a sharp change in surface activity at this concentration. This is in the vicinity of the reported value of 0.1 mg/mL[64]. Below this concentration, the surface activity is that of pure water 72 mJ/m^2. Above this concentration, the surface tension drops dramatically to 60 mJ/m^2 and is maintained at this level at higher concentrations. The advantage of using highly purified peptide is that a surface tension 'dip' is not observed, thus making CAC determination more readily discernable.

The assembly of EAK16-II is confirmed when its nanostructures are visualized by AFM on a mica surface. The AFM images show two distinct types of nanostructures - globular aggregates and fibre formations (Figure 4-3). Fibre formation is observed at concentrations above the CAC. At low peptide concentrations, below the CAC, globular aggregates are observed. It has been previously reported that at low concentrations that both globular and fibrils were observed below the CAC[98]. This may be attributed to the impurities in the solution functioning as seeds, which can initiate the nucleation process for further aggregation.

5.2. Crude Peptide

The impurity effect is evident in the equilibrium surface tension profile of the crude peptide solutions. At low concentrations of 0.01 and 0.03 mg/mL the surface tension is similar to that of water as seen for the high purity peptide. However, at 0.05 and 0.07mg/mL, the surface tension drops dramatically to around 55 mJ/m^2 before increasing to approximately 58 mJ/m^2 at higher concentrations.

The formation of nuclei is expected to depend on concentration. At concentrations above the CAC, nuclei are generated by the self-association of EAK16-II molecules. Below the CAC, impurities in solution may function as seeds (or nuclei) to induce assembly. The presence of impurities is confirmed by the depression observed in the surface tension measurements (Figure 4-2). The presence of impurities is also noticed in the aggregation of the crude peptide. As reported previously, both globular and fibrils are observed below the CAC. The existence of aggregates at this concentration is believed to be the result of impurities that act as seeds for the formation of fibre-like structures (Figure 4-4). Above the CAC, fibre networks and membrane-like structures are observed.

5.3 Surface Tension 'Dip'

The presence of the surface tension 'dip' has been observed previously in surfactant systems[85-94]. The observed trend may be used to explain the seeding effect on EAK16-II peptide assembly. The system must include small but surface active and easily solubilized components. At concentrations less than the CAC, such components lower the surface tension below that of the pure peptide because of its higher surface activity. The impurity and the peptide form assemblies that appear at lower concentrations than those of the pure peptide. The impurities are

depleted in the solution and the surface by the peptide assemblies because they are readily incorporated into the nano- or microstructures. The surface tension is thus raised effectively to the value of the pure peptide.

The crude peptide used in these experiments was produced under Fmoc solid phase synthesis. The impurities found in the non-purified peptide may include deleted sequences, truncated sequences, incompletely deprotonated sequences, DTT (dithiothreitol), TFA (trifluoroacetic acid) and acetic acid. The majority of the impurities are truncated sequences such as EAK4, EAK8, and also amino acid monomers. Thus, these components should be among the first to be investigated to better understand the seeding phenomena.

5.4 Amino Acid Seeding Agents

The impurities selected in this study to better understand the seeding effect were alanine, glutamic acid and lysine. These amino acids constitute the basic residues in the EAK16-II sequence. These L-amino acids differ in size, structure and charge with molecular weights of 89.09, 147.13 and 146.19 g/mol, respectively. Contrary to previous perceptions about the nature of the seeding impurities alanine, glutamic acid and lysine amino acids by themselves are not highly surface active (Figure 4-5). Thus, if these compounds are able to induce a surface tension dip as seen in the crude peptide sample, then a synergistic effect must exist between the seeding agent and the peptide. From the molecular conformation studies performed on EAK16-II, the seeding agent may be responsible for transforming peptide molecule from the stretched conformation to a hairpin structure (Figure 5-1a). These structures may act as nuclei for the formation of nanostructure assemblies.

It should be noted that the true amount of EAK16-II in crude peptide samples at any given concentration would be less than that of high purity peptide samples. This occurs because the crude peptide also contains amounts of truncated sequences and reagents used in the synthesis process. However, since the purity level of the crude sample is highly variable (~20%), simulating the crude composition or relative impurity would be problematic. Alternatively, the seeding agents were added to the high purity peptide on a molar basis to determine their effect on peptide activity and morphology. The 0.07 mg/mL peptide concentration was used to evaluate the seeding agents since the dip appeared at this concentration in the crude peptide (Figure 4.2).

5.5 Alanine

The effect of the alanine seeding agent was determined by varying its molar ratio in 0.07 mg/mL high purity EAK16-II solutions (Figure 4-6). The equilibrium surface tension is shown to decrease even at a 1:50 alanine-to-peptide ratio to 68.5 mJ/m^2. This is substantially less than the value of water (72.5 mJ/m^2). At higher molar ratios, the surface tension reduces to a minimum of about 59.5 mJ/m^2 at a 10:1 ratio. This suggests a synergistic effect between the alanine and the peptide since these compounds alone yield a surface tension similar to that of water. However, above a 10:1 seeding ratio, the equilibrium surface tension begins to increase. At the high molar ratios the amount of alanine greatly dominated the relative amount of peptide. The excess alanine may shield the peptide from the air-water interface and increase the time required for the peptide to migrate to the surface.

From dynamic surface tension data, some information can be attained by examining the induction time. When the concentration of peptide is sufficiently low, the surface tension does not change within an initial period. This time is referred to as the induction time. This

phenomenon exists in most biomolecular systems, and many mechanisms have been proposed to explain it. One proposed theory for the kinetics of globular protein adsorption is based on a diffusion model[100]. According to this theory, the induction time represents the time required for the surface monolayer to attain a certain minimum coverage, above which the surface tension is reduced.

The induction period observed for the alanine and peptide solutions suggests that the increase in alanine-to-peptide ratio increases the surface activity of the nanoparticles (Figure 4-7). The induction time is the measure of the time required for a surfactant to modify the air-water interface. A newly created pendant drop has an initial surface tension equal to that of pure water. With time, hydrophobic materials will migrate to the air-water interface. Small particles move quickly but a large number of these particles are required to modify the solution interface, alternatively large particles move more slowly. The increase in the alanine:EAK ratio to 10:1 decreases the induction time. The alanine may be increasing the hydrophobic character of the peptide particles (Figure 5-1b). At higher alanine seeding ratios, the amount of peptide in solution is saturated by alanine monomers, which may shield the peptide from the air-water interface.

Interestingly, the AFM results indicate that the seeding ratio required for fibre formation is in the 10:1 region (Figure 4-8). This suggests that there are two processes that are taking place. The first is seeding, where the presence of impurities induces fibre formation (Figure 5-1a). The second is surface modification where amino acids accumulate at the surface of aggregated peptide and modify its surface activity (Figure 5-1b). This would explain the appearance of fibres at low seeding ratios with the absence of any change in the surface tension. This suggests

that at low seeding ratios, the seeding agents will predominantly function to induce fibre formation. At higher seeding ratios, these agents act to enhance the activity of the nanoparticles.

The ability of the alanine seeding agent to induce a surface tension 'dip' was examined by adding alanine at the 10:l seeding ratio to peptide concentrations above and below the CAC. Since the impurity in a purchased peptide sample is presumed to be uniform, the impurity ratio should remain the same for all concentrations. The alanine seeding ratio of 10:1 produced a surface tension drop to 60 mJ/m^2 at a 0.07 mg/mL peptide concentration. This did not produce the surface tension dip expected when the effects of lower and higher concentrations were examined (Figure 4-9). There was a general decrease in the surface tension at the lower concentrations. This supports the idea that the alanine may have amplified the surface activity of the peptide particles. This is seen at the 0.03 mg/mL concentration as the surface tension is lowered to 65.5 mJ/m^2, which is lower that that observed for the crude or high purity peptide alone.

The morphology of the peptide aggregates is influenced by the presence of the alanine seeding agent (Figure 4-10). At 0.03 mg/mL, short fibrils are formed. This suggests that the addition of alanine at the 10:1 ratio can induce fibre formation at low concentrations. At higher peptide concentrations fibre and membrane-like structures are observed.

5.6 Glutamic Acid

The glutamic acid monomer was shown to decrease the equilibrium surface tension of 0.07 mg/mL high purity peptide to a minimum at the 10:1 seeding ratio (Figure 4-11). The equilibrium surface tension drops drastically at the 1:1 ratio and reaches a minimum value of 55.5mJ/m^2 at the 10:1 seeding ratio. This surface tension drop is much more pronounced than

that observed for alanine. This may be due to the long carbon chain structure of glutamic acid relative to alanine (Figure 5-1c). This may give glutamic acid a larger hydrophobic region to greatly influence the peptide surface tension. At the 10:1 ratio, the surface tension value is similar to that seen for the crude peptide at the same peptide concentration. At higher seeding ratios, the surface tension begins to increase as seen with alanine seeding. This may be a result of the glutamic acid monomers shielding the peptide from the surface. Thus, this may be attributed to the abundance of glutamic acid or rather the reduction in the relative amount of peptide in solution. The induction time also shows a minimum at 10:1 seeding ratio (Figure 4-12). Furthermore, the morphology of the peptides shows that the fibre formation is predominant in the 10:1 seeding ratio region (Figure 4-13).

A surface tension dip was generated using the 10:1 glutamic acid to peptide seeding ratio at concentrations around the CAC (Figure 4-14). This indicates that glutamic acid can simulate the dip phenomenon indicative of the presence of impurities. The lower surface tension 'dip' correlates well with formation of fibres (Figure 4-15). At higher concentrations, larger peptide aggregates form and envelope the monomers and reduce their surface activity. This may account for the surface tension increases above a 0.07mg/mL concentration.

5.7 Lysine

The lysine represents a seeding agent that is positively charged and has a larger chain length than the other amino acids. When combined with 0.07 mg/mL peptide at various molar ratios, a minimum surface tension value of about 54 mJ/m^2 is achieved at a 1:1 molar ratio (Figure 4-16). This is also confirmed with the induction time (Figure 4-17) and AFM results (Figure 4-18). The induction time appears more sensitive to the presence of lysine than the other

seeding agents. At the 1:10 molar ratio the induction time decreases to less that 5000 sec much lower that the other impurities. There appears to be a larger region in which the induction time is decreased below the 5000 sec mark. The fibre formation was dominant around the 10:1 molar ratio.

The 10:1 lysine-to-peptide molar ratio was found to be able to produce a 'dip' in the surface tension versus concentration curve that most resembles the crude peptide (Figure 4-19). At 0.07 mg/mL the surface tension decreases to about 54.5 mJ/m^2. However, at higher concentrations the surface activity of the pure peptide is expressed. Interestingly, at the low concentration of 0.03 mg/mL a more hydrophobic character is observed.

The morphologies found in the lysine peptide differed from those seen with alanine or glutamic acid systems. As shown in Figure 4-20, fibres are formed at concentrations around 0.07 mg/mL. At the 0.07 mg/mL concentration, these fibres appear much thicker. At the high concentration of 0.3 mg/mL a membrane-like structure forms. This suggests that lysine assists in peptide assembly and the formation of membrane-like structures.

For all the amino acid seeding agents examined the 10:1 seeding ratio appears to have some significance. Interestingly, when converted to a mass basis, the 10:1 molar ratio represents approximately 35 wt% impurity. This coincides with the 65% purity level estimated for the crude sample. The same trend is seen above the 10:1 ratio as the surface tension begins to rise minimizing the importance of the peptide in the solution.

The presence of impurities or seeding agents can induce the assembly of peptides below the CAC. However, the effect of the peptide assembly is influenced by the nature of the seeding agent. Smaller seeding agents such as alanine will have less of an effect than larger charged molecules such as glutamic acid and lysine. The seeding agent has two effects on peptide

assembly. The first effect is to induce assembly at low concentrations (Figure 5-1a). This is beneficial for applications where the effectivness of small amounts of peptide can be maximized. This may have applications in drug coatings where the seeding agent may be a therapeutic agent. In that case, the therapeutic may be encased within a single peptide fibre as opposed to being coated by fibre networks.

A

B

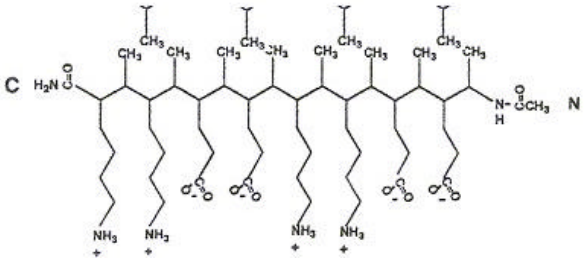

C

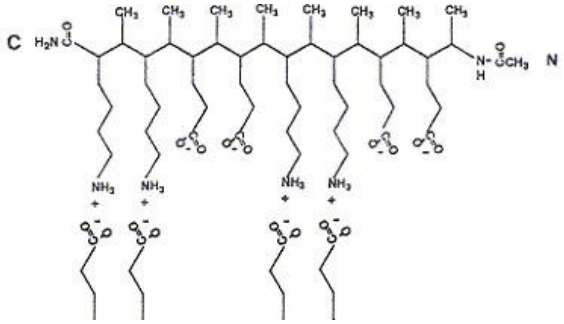

D

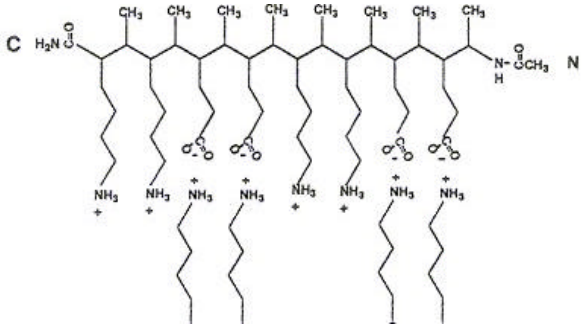

Figure 5-1 Schematic of interactions of EAK16-II and Impurities. (a) the presence of impurities act as seeding agents to favour coiled peptide structure. The addition of imputities may interact with the peptide residues (b) alalnine intercalating in hydrophonbic regions (c) glutamic acid monomers ionic attraction to lysine resides (d) lysine monomers ionic attraction to glutamic acid residues. This schematic indicates that a peptide-to-imputiry ration between 1:1 and 1:10 may be of stochiometric significance.

The second effect, involving surface modification of nanostructures, is seen at higher seeding ratios such as the 10:1 molar ratio. Here, the excess seeds act not only as nuclei for peptide assembly but also to modify the surface activity of the peptide particles. The seeding agents may act to amplify the hydrophobic (or hydrophilic) nature of the peptide assemblies. Alanine, through hydrophobic interactions can increase the hydrophobicity of peptide assemblies (Figure 5-1b). Alternatively, the glutamic acid and lysine seeding agents can utilize ionic interactions with complementary residues on the peptide chain as shown in Figure 5-1c and Figure F-1d, respectively. The glutamic acid and lysine amino acids would then mask the ionic component of the peptide with their relatively hydrophobic carbon chain.

The assembly process and activity of EAK16-II can be influenced by the presence of seeding agents. This may be an important characteristic in the application of EAK16-II to fields such as drug delivery or understanding conformation diseases.

6.0 CONCLUSIONS AND RECOMMENDATIONS

6.1 Conclusions

The effect of seeding agent on the assembly of EAK16-II was studied by incorporating alanine, glutamic acid, or lysine at low peptide concentrations. Surface tension provided information about the surface activity while AFM imaging provided visual verification of fibre formation to study the seeding effect on peptide assembly. The following conclusions are drawn:

1. The CAC of EAK16-II was verified to be within the range 0.09-0.1 mg/mL.
2. The presence of impurities is responsible for the surface tension ‘dip’ observed in crude EAK16-II.
3. The effectiveness of the seeding agents follow the trend K>E>A. This trend is related to the molecular structure of these seeding agents.
4. Glutamic acid and lysine seeding agents were able to simulate the ‘dip’ at 0.07 mg/mL peptide concentration seen in the crude peptide.
5. Seeding agents can be used for two purposes. The first is to induce assembly below the critical aggregation concentration of the peptide. The second is to modify the surface activity of the assembled peptide particles.

6.2 Recommendations

To better understand the seeding phenomenon, several directions and methods could be adopted in the future.

1. Determine if the peptides formed by seeding mechanism posses the same stability as peptides formed above the CAC. This may result in method of controlling the stability of peptide assemblies and may provide a way of engineering peptide material with desired half-lives.

2. The peptide morphologies are often irregular making it difficult to accurately characterize the dimensions of peptide assemblies. A strict protocol for quantitative assessment of the peptide assembles should be investigated.

3. Further tests using other reagents used in the synthesis of EAK 16-II and truncated sequences such as EAK8.

4. Find a relationship between the molecular conformation of the peptide and the assembled structure. This will lead to a better understanding of the assembly process.

5. Other effects such as temperature can be studied to help understand the self-assembly mechanism. Reducing the temperature of peptide solutions may enable analysis of time course of peptide assembly.

6. Apply seeding mechanism for coating of therapeutic material and/or modify the surface characteristic of the assembled particles.

7.0 REFERENCES

1. Merkle,R.C. Biotechnology as a route to nanotechnology. *Trends Biotechnol.* **17**, 271-274 (1999).

2. Stupp,S.I. & Braun,P.V. Molecular manipulation of microstructures: biomaterials, ceramics, and semiconductors. *Science* **277**, 1242-1248 (1997).

3. Alper,J. Chemists look to follow biology lead. *Science* **295**, 2396-2397 (2002).

4. Service,R.F. Can chemists assemble a future for molecular electronics? *Science* **295**, 2398-2399 (2002).

5. Lowe,C.R. Nanobiotechnology: the fabrication and applications of chemical and biological nanostructures. *Curr. Opin. Struct. Biol.* **10**, 428-434 (2000).

6. Seeman,N.C. & Belch,A.M. Emulating biology: building nanostructures from the bottom up. *Proc. Natl. Acad. Sci. USA* **99**, 6451-6455 (2002).

7. Lawrence,R.N. James Gimzewski Discusses the potential of nanobiotechnology. *Drug Discov. Today* **7**, 18-21 (2002).

8. Service,R.F. Molecules get wired. *Science* **294**, 2442-2443 (2001).

9. Hench,L.L. & Polak,J.M. Third - generation biomedical materials. *Science* **295**, 1014-1017 (2002).

10. Zhang,S. Encyclopedia of materials: sciene and technology. Buschow,K.H.J. *et al.* (eds.), pp. 5822-5829 (Elsevier, Oxford,2001).

11. Whitesides,G.M., Mathias,J.P. & Seto,C.T. Molecular self-assembly and nanochemistry: a chemical strategy for the synthesis of nanostructures. *Science* **254**, 1312-1319 (1991).

12. Zhang,S. Fabrication of novel biomaterials through molecular self-assembly. *Nature Biotech.* **21**, 1171-1178 (2003).

13. Zhang,S., Marini,D.M., Hwang,W. & Santoso,S. Design of nanostructured biological materials through self-assembly of peptides and proteins. *Curr. Opin. Chem. Biol.* **6**, 865-871 (2002).

14. Santoso,S.S., Vauthey,S. & Zhang,S. Structures, function and applications of amphiphilic peptides. *Curr. Opin. Coll. Inter. Sci.* **7**, 262-266 (2002).

15. Zhang,S. Emerging biological materials through molecular self-assembly. *Biotechnol. Adv.* **20**, 321-339 (2002).

16. Lynn,D.G. & Meredith,S.C. Review: model peptides and the physicochemical approach to β-amyloids. *J. Struct. Biol.* **130**, 153-173 (2000).

17. Rochet,J.-C. & Lansbury Jr,P.T. Amyloid fibrillogenesis: themes and variations. *Curr. Opin. Struct. Biol.* **10**, 60-68 (2000).

18. Mutter,M. & Hersperger,R. Peptides as conformational switch: medium-induced conformational transitions of designed pepitdes. *Angew. Chem. Int. Ed. Engl.* **29**, 185-187 (1990).

19. Mutter,M., Gassmann,R., Buttkus,U. & Altmann,K.-H. Switch peptides: pH-Induced α-helix to β-sheet transtions of bis-amphiphilic oligopeptides. *Angew. Chem. Int. Ed. Engl.* **30**, 1514-1516 (1991).

20. Zhong,L. & Johnson Jr,W.C. Environment affects amino acid preference for secondary structure. *Proc. Natl. Acad. Sci. USA* **89**, 4462-4465 (1992).

21. Cerpa,R., Cohen,F.E. & Kuntz,I.D. Conformational switching in designed peptides: the helix/sheet transition. *Fold. Des.* **1**, 91-101 (1996).

22. Fukushima,Y. Sequence effects on helix-sheet conformational transitions of designed amphiphilic pepitdes. *Bull. Chem. Soc. Jpn.* **69**, 701-708 (1996).

23. Zhang,S., Lockshin,C., Herbert,A., Winter,E. & Rich,A. Zoutin, a putative Z-DNA binding protein in *Saccharomyces cerevisiae*. *EMBO. J.* **11**, 3787-3796 (1992).

24. Pennisi,E. Material peptide. *Science News* **143**, 316-317 (1993).

25. Zhang,S., Holmes,T., Lockshin,C. & Rich,A. Spontaneous assembly of a self-complementary oligopeptide to form a stable macroscopic membrane. *Proc. Natl. Acad. Sci. USA* **90**, 3334-3338 (1993).

26. de la Paz,M.L. *et al. De novo* designed peptdie-based amyloid fibrils. *Proc. Natl. Acad. Sci. USA* **99**, 16052-46057 (2002).

27. Hong,Y., Legge,R.L., Zhang,S. & Chen,P. Effect of amino acid sequence and pH on Nanofiber formation with self-assembling peptides EAK16-II and EAK16-IV. *Biomacromolecules* **4**, 1433-1442 (2003).

28. Niece,K.L., Hartgerink,J.D., Donners,J.J.J.M. & Stupp,S.I. Self-assembly combining two bioactive peptide-amhpiphile molecules into nanofibers by electrostatic attraction. *J. Am. Chem. Soc.* **125**, 7146-7147 (2003).

29. Leon,E.J., Verma,N., Zhang,S., Lauffenburger,D.A. & Kamm,R.D. Mechanical properties of a self-assembling oligopeptide matrix. *J. Biomater. Sci. Polymer Edn.* **9**, 297-312 (1998).

30. Caplan,M.R., Schwartzfarb,E.M., Zhang,S., Kamm,R.D. & Lauffenburger,D.A. Effects of systematic variation of amino acid sequence on the mechanical properties of a self-assembling, oligopeptide biomaterial. *J. Biomater. Sci. Polymer Edn.* **13**, 225-236 (2002).

31. Zhang,S., Lockshin,C., Cook,R. & Rich,A. Unusually stable β-sheet formation in an ionic self-complementary oligopeptide. *Biopolymers* **34**, 663-672 (1994).

32. Zhang,S. & Altman,M. Peptide self-assembly in functional polymer science and engineering. *Reactive and Functional Polymers* **41**, 91-102 (1999).

33. Aggeli,A. *et al.* Hierarchical self-assembly of chiral rod-like molecules as a model for peptide β-sheet tapes, ribbons, fibrils, and fibers. *Proc. Natl. Acad. Sci. USA* **98**, 11857-11862 (2001).

34. Waterhous,D.V. & Johnson Jr,W.C. Importance of environment in determining secondary structure in proteins. *Biochemistry* **33**, 2121-2128 (1994).

35. Caplan,M.R., Schwartzfarb,E.M., Zhang,S., Kamm,R.D. & Lauffenburger,D.A. Control of self-assembling oligopeptide matrix formation through systematic variation of amino acid sequence. *Biomaterials* **23**, 219-227 (2002).

36. Altman,M., Lee,P., Rich,A. & Zhang,S. Conformational behavior of ionic self-complementary peptides. *Protein Sci.* **9**, 1095-1105 (2000).

37. Sipe,J.D. & Cohen,A.S. Review: history of the amyloid fibril. *J. Struct. Biol.* **130**, 88-98 (2000).

38. Santoso,S. & Zhang,S. Encyclopedia of Nanoscience and Nanotechnology. Nalwa,H.S. (ed.) (American Scientific Publishers, Stevenson Ranch, CA,2003).

39. Aggeli,A., Boden,N. & Zhang,S. Self-assembly of peptides in medicine: two sides of the coin. *Mol. Med. Today* **5**, 512-513 (1999).

40. McCutchen,S.L., Lai,Z., Miroy,G.J., Kelly,J.W. & Colon,W. Comparison of lethal and nonlethal Transthyretin variants and their relationship to amyloid disease. *Biochemistry* **34**, 13527-13536 (1995).

41. Lai,Z., Colon,W. & Kelly,J.W. The acid-mediated denaturation pathway of transthyretin yields a conformational intermediate that can self-assemble into amyolid. *Biochemistry* **35**, 6470-6482 (1996).

42. Halverson,K., Fraser,P.E., Kirschner,D.A. & Lansbury Jr,P.T. Molecular determinants of amyloid deposition in Alzheimer's disease: conformational studies of synthetic β-protein fragments. *Biochemistry* **29**, 2639-2644 (1990).

43. Walsh,D.M. *et al.* Amyloid β-protein fibrillogenesis. *J. Biol. Chem.* **274**, 25945-25952 (1999).

44. Benzinger,T.L.S. *et al.* Two-dimensional structure of β-amyloid(10-35) fibrils. *Biochemistry* **39**, 3491-3499 (2000).

45. Burkoth,T.S. *et al.* Structure of the β-amyloid$_{(10\text{-}35)\ \text{fibril}}$. *J. Am. Chem. Soc.* **122**, 7883-7889 (2000).

46. Zou,W.-Q., Yang,D.-S., Fraser,P.E., Cashman,N.R. & Chakrabartty,A. All or none fibrillogenesis of a prion peptide. *Eur. J. Biochem.* **268**, 4885-4891 (2001).

47. Fandrich,M., Fletcher,M.A. & Dobson,C.M. Amyloid fibrils from muscle myoglobin. *Nature* **410**, 165-166 (2001).

48. West,M.W. *et al. De novo* amyloid proteins from designed combinatorial libraries. *Proc. Natl. Acad. Sci. USA* **96**, 11211-11216 (1999).

49. MacPhee,C.E. & Dobson,C.M. Formation of mixed fibrils demonstrates the generic nature and potential utility of amyloid nanostructures. *J. Am. Chem. Soc.* **122**, 12707-12713 (2000).

50. Pandya,M.J. *et al.* Sticky-end assembly of a designed peptide fiber provides insight into protein fibrillogenesis. *Biochemistry* **39**, 8728-8734 (2000).

51. Iconomidou,V.A. *et al.* Amyloid-like fibrils from an 18-residue peptide analogue of a part of the central domain of the B-family of silkmoth chorion proteins. *FEBS Lett.* **499**, 268-273 (2001).

52. Gosal,W.S., Clark,A.H., Pudney,P.D. & Ross-Murphy,S.B. Novel amyloid fibrillar networks derived from a globular protein: β-Lactoglobulin. *Langmuir* **18**, 7174-7181 (2002).

53. Ohnishi,S., Koide,A. & Koide,S. The roles of turn formation and cross-strand interactions in fibrillization of peptides derived from the OspA single-layer β-sheet. *Protein Sci.* **10**, 2083-2092 (2001).

54. Koga,T., Taguchi,K., Kobuke,Y., Kinoshita,T. & Higuchi,M. Structural regulation of a peptide-conjugated graft copolymer: a simple model for amyloid formation. *Chem. Eur. J.* **9**, 1146-1156 (2003).

55. Ogihara,N.L. *et al.* Design of three-dimensional domain-swapped dimers and fibrous oligomers. *Proc. Natl. Acad. Sci. USA* **98**, 1404-1409 (2001).

56. Ghanta,J., Shen,C.-L., Kiessling,L.L. & Murphy,R.M. A strategy for designing inhibitors of β-amyloid toxicity. *J. Biol. Chem.* **271**, 29525-29528 (1996).

57. Hardy,J. & Selkoe,D.J. The amyloid hypothesis of Alzheimer's disease: progress and problems on the the road to therapeutics. *Science* **297**, 353-356 (2002).

58. Xiong,H., Buckwalter,B.L., Shieh,H.-M. & Hecht,M.H. Periodicity of polar and nonpolar amino acids is the major determinant of secondary structure in self-assembling oligomeric peptides. *Proc. Natl. Acad. Sci. USA* **92**, 6349-6353 (1995).

59. Aggeli,A. *et al.* Responsive gels formed by the spontaneous self-assembly of peptides into polymeric β-sheet tapes. *Nature* **386**, 259-262 (1997).

60. Nowak,A.P. *et al.* Rapidly recovering hydrogel scaffolds from self-assembling diblock copolypeptide amphiphiles. *Nature* **417**, 424-428 (2002).

61. Zhang,S. *et al.* Biological surface engineering: a simple system for cell pattern formation. *Biomaterials* **20**, 1213-1220 (1999).

62. Good,T.A. & Murphy,R.M. Aggregation state-dependent binding of β-amyloid peptide to protein and lipid components of rat cortical homogenates. *Biochem. Biophys. Res. Comm.* **207**, 209-215 (1995).

63. Fraser,P.E. *et al.* Conformation and fibrillogenesis of Alzheimer Aβ peptides with selected substitution of charged residues. *J. Mol. Biol.* **244**, 64-73 (1994).

64. Fung,S.Y., Keyes,C., Duhamel,J. & Chen,P. Concentration effect on the aggregation of a self-assembling oligopeptide. *Biophys. J.* **85**, 537-548 (2003).

65. Jun,S. *et al.* Self-assembly of the ionic peptide EAK16: the effect of charge distributions on self-assembly. Biophys.J. 2003.

66. Hong,Y., Legge,R.L., Zhang,S. & Chen,P. Effect of amino acid sequence and pH on nanofiber formation of self-assembling peptides EAK16-II and EAK16-IV. *Biomacromolecules* **4**, 1433-1442 (2003).

67. Dhadwar,S.S., Bemman,T., Anderson,W.A. & Chen,P. Yeast cell adhesion on oligopeptde modified surfaces. *Biotechnol. Adv.* **21**, 395-406 (2003).

68. Holmes,T.C. *et al.* Extensive neurite outgrowth and active synapse formation on self-assembling peptide scaffolds. *Proc. Natl. Acad. Sci. USA* **97**, 6728-6733 (2000).

69. Jun,S. *et al.* Self-assembly of the ionic peptide EAK16: the effect of charge distributions on self-assembly. *Biophys. J.* **87**, 1249-1259 (2004).

70. Benaki,D.C. *et al.* Laser-Raman and FT-IR spectroscopic studies of peptide-analogues of silkmoth chorion protein segments. *Int. J. Biol. Macromol.* **23**, 49-59 (1998).

71. Schulz,G.E. & Schirmer,R.H. Principles of protein structure. Springer-Verlag New York Inc., New York (1979).

72. Zhang,S. & Egli,M. A proposed complementary pairing mode between single-stranded nucleic acids and β-stranded peptides: a possible pathway for generating complex biological molecules. *Complexity* 49-55 (1995).

73. Zhang,S. *et al.* Self-complementary oligopeptide matrices support mammalian cell attachment. *Biomaterials* **16**, 1385-1393 (1995).

74. Clint,J.H. Surfactant aggregation. Blackie & Son Ltd., New York (1992).

75. Harper,J.D. & Lansbury Jr,P.T. Models of amyloid seeding in Alzheimer's disease and scarpie: mechanistic truths and physiological consequences of the time-dependent solubility of amyloid proteins. *Annu. Rev. Biochem.* **66**, 385-407 (1997).

76. Kelly,J.W. The alternative conformations of amyloidogenic proteins and their multi-step assembly pathways. *Curr. Opin. Struct. Biol.* **8**, 101-106 (1998).

77. Zhao,X., Vistakula,K.K., Uematsu,T., Zelman,A.K. & Zhang,S. MRS Symposium Proceedings . 2003 In press.

78. Lomakin,A., Chung,D.S., Benedek,G.B., Kirschner,D.A. & Teplow,D.B. On the nucleation and growth of amyloid β-protein fibrils: detection of nuclei and quantitation of rate constants. *Proc. Natl. Acad. Sci. USA* **93**, 1125-1129 (1996).

79. Lomakin,A., Teplow,D.B., Kirschner,D.A. & Benedek,G.B. Kinetic theory of fibrillogenesis of amyloid β-protein. *Proc. Natl. Acad. Sci. USA* **94**, 7942-7947 (1997).

80. Fields,G.B. & Noble,R.L. Solid phase peptide synthesis utilizing 9-fluorenylmethoxycarbonyl amino acids. *Int. J. Peptide Protein Res.* **35**, 161-214 (1990).

81. Barany,G., Kneib-Cordonier,N. & Mullen,D.G. Solid-phase peptide synthesis: a silver anniversary report. *Int. J. Peptide Protein Res.* **30**, 705-739 (1987).

82. Bodanszky,M. Principles of peptide synthesis. NY (1993).

83. Jonsson,B., Lindman,B., Holmberg,K. & Kronberg,B. Surfactants and poly,ers in aqueous solution., pp. 249-264 (John Wiley & Sons Ltd., NY,1998).

84. Colinet,P., Legtos,J.C. & Velarde,M.G. Nonlinear dynamics of surface-tension-driven instabilities. Wiley-VCH, Berlin (2001).

85. Persson,C.M., Claesson,P.M. & Lunkenheimer,K. Interfacial behavior of n-Decyl-β-D-maltopyranoside on hydrophobic interfaces and the effect of small amounts of surface-active impurities. *J. Colloid Interface Sci.* **251**, 182-192 (2002).

86. Liu,X.Y. Interficial effect of molecules on nucleation kinetics. *J. Phys. Chem.* **105**, 11550-11558 (2001).

87. Henderson,D.C. & Micale,F.J. Dynamic surface tension measurements with the drop mass technique. *J. Colloid Interface Sci.* **158**, 289-294 (1993).

88. Priester,T., Bartoszek,M. & Lunkenheimer,K. Influence of surface-active trace impurities on the surface properties of aqueous solutions of oligoethylene glycol monooctyl ethers. *J. Colloid Interface Sci.* **208**, 6-13 (1998).

89. Gol'dshtein,R.V. & Sarychev,M.E. Surface tension at the interface of materials as a function of impurity content. *MAIK* **385**, 621-624 (2002).

90. Miles,G.D. & Shedlovsky,L. Minima in surface tension-concentration curves od solutions of sodium alcohol sulphates. *Acc. Chem. Res* 57-62 (1943).

91. Miles,G.D. Minima in surface tension and interfacialtension curves. *Acc. Chem. Res* 71-76 (1944).

92. Mysels,K.J. & Florence,A.T. The effect of impurities on dynamic surface tension - basis for a valaid surface purity criterion. *J. Colloid Interface Sci.* **43**, 577-582 (1972).

93. Warszynski,P., Lunkenheimer,K. & Czichocki,G. Effect of counterions on the adsorption of ionic surfactants at fluid-fluid interfaces. *Langmuir* **18**, 2506-2514 (2002).

94. Wood,S.J. *et al.* Alpha-Synuclein Fibrillogenesis is nucleation-dependant. *J. Biological Chemistry* **274**, 19509-19512 (1999).

95. Oliva,M. *et al.* Self-assembly of drug-polymer complexes: A spontaneous nanoencapsulation process monitored by atomic force microscopy. *journal of pharmaceutical sciences* **92**, 77-83 (2003).

96. Allcock,H.R. & Lampe,F.W. Contemporary polymer chemistry. Prentice-Hall, Inc., Englewood Cliffs (1990).

97. Lahooti,S., Del Rio,O.I., Neumann,A.W. & Cheng,P. Applied surface thermodynamics. Neumann,A.W. & Spelt,J.K. (eds.), pp. 441-507 (Marcel Dekker, Inc., New York,1996).

98. Fung,S.Y., Hong,Y., Dhadwar,S.S., Zhao,X. & Chen,P. Handbook of nanostructured biomaterials and their applications. Nalwa,H.S. (ed.), 2004. In press.

99. Cabrerizo-Vilchez,M.A., Policova,Z., Kwok,D.Y. & Chen,P. The temperature dependance of teh interficial tension of aqueous human albumin solution/decane. *Colloids Surf. B: Biointerfaces* **5**, 1-9 (1995).

100. Miller,R., Aksenenko,E.V., Fainerman,V.B. & Pison,U. Kinetics of adsorption of globular proteins at liquid/fluid interfaces. *Colloids Surf. A: Physicochemical and Engineering Aspects* **183**, 381-390 (2001).